

# Structural Symmetry in Membrane Proteins\*

Lucy R. Forrest

Computational Structural Biology Group, Porter Neuroscience Center, National Institute of Neurological Disorders and Stroke, National Institutes of Health, Bethesda, Maryland 20852; email: lucy.forrest@nih.gov

Annu. Rev. Biophys. 2015. 44:311–37

The *Annual Review of Biophysics* is online at [biophys.annualreviews.org](http://biophys.annualreviews.org)

This article's doi:

10.1146/annurev-biophys-051013-023008

\*This is a work of the US Government and is not subject to copyright protection in the United States.

## Keywords

oligomer, internal repeats, inverted-topology repeats, asymmetry, alternating access

## Abstract

Symmetry is a common feature among natural systems, including protein structures. A strong propensity toward symmetric architectures has long been recognized for water-soluble proteins, and this propensity has been rationalized from an evolutionary standpoint. Proteins residing in cellular membranes, however, have traditionally been less amenable to structural studies, and thus the prevalence and significance of symmetry in this important class of molecules is not as well understood. In the past two decades, researchers have made great strides in this area, and these advances have provided exciting insights into the range of architectures adopted by membrane proteins. These structural studies have revealed a similarly strong bias toward symmetric arrangements, which were often unexpected and which occurred despite the restrictions imposed by the membrane environment on the possible symmetry groups. Moreover, membrane proteins disproportionately contain internal structural repeats resulting from duplication and fusion of smaller segments. This article discusses the types and origins of symmetry in membrane proteins and the implications of symmetry for protein function.

## Contents

INTRODUCTION .....	312
FUNCTIONS OF MEMBRANE PROTEINS .....	312
Receptors .....	312
Channels and Transporters .....	313
Membrane Enzymes .....	313
Cofactor Scaffolding Proteins .....	313
FUNCTIONAL DIVERSITY, PROTEIN SIZE, AND SYMMETRY .....	314
Oligomerization .....	314
Gene Fusion .....	314
Internal Repeats .....	315
SYMMETRY IN MEMBRANE PROTEIN STRUCTURES .....	320
Nonsymmetric Membrane Proteins .....	320
Cyclic Symmetry .....	320
Dihedral and Plane Symmetries .....	328
Higher-Order Cubic and Space-Group Symmetries .....	329
Dynamic Transitions Between Symmetry Types .....	329

## INTRODUCTION

Symmetry, defined as the property of having the same appearance from two or more vantage points, is an aesthetically appealing and common feature of natural systems (52). In the structure of macromolecules and, in that of proteins in particular, researchers have identified a multitude of symmetries and pseudosymmetries, which appear to have a range of functional advantages (50, 70). As we reach the milestone of identifying 500 unique structures of membrane proteins (112, 155, 161), reviewing the prevalence and mechanistic significance of symmetry in this special class of proteins seems timely.

After briefly introducing the major functional classes of integral membrane proteins, I discuss the emergence of symmetry in their structures as a result of gene duplication or oligomerization. I then describe the specific types of symmetry observed thus far, as well as their mechanistic implications. This discussion focuses on membrane proteins with chains spanning the entire lipid bilayer one or more times [in contrast to monotopic, membrane-associated proteins (13, 155)]. I conclude with open questions and exciting future directions for the field.

## FUNCTIONS OF MEMBRANE PROTEINS

Approximately 25–35% of the genes in a genome encode for integral membrane proteins (3, 81, 123). These proteins perform a wide variety of functions that can be grouped into four types: receptors, channels and transporters, enzymes, and cofactor scaffolds.

### Receptors

Lipid bilayers serve as hydrophobic barriers that protect the interior of cells and organelles, but they also impede numerous essential processes. So-called receptor proteins facilitate the transmission of information across membranes. In response either to light or to chemical signals from the exterior of the cell, these proteins adopt different states or conformations and thereby

modulate their ability to interact with other proteins in the interior of the cell. The family of seven-transmembrane (TM)-helix G protein-coupled receptors (GPCRs) is the most prominent example, and it constitutes the largest functional class in eukarya (3). Receptor tyrosine kinases (RTKs) comprise another large and important family of membrane proteins in this class (83).

---

**Domain:** a functional and structural unit of protein, typically between 100 and 250 amino acids in length

---

## Channels and Transporters

The second-most abundant membrane proteins, accounting for between 2 and 15% of the genes in a given genome (3, 5), are those that facilitate selective passage of chemicals across the lipid membrane. In the simplest case, proteins called channels create pores through which ions and other molecules diffuse passively, that is, down their concentration gradients. To regulate this process, many channels incorporate so-called gating mechanisms that respond to environmental stimuli such as voltage or ligand binding.

Cells also need to expel toxic compounds and to take up rare nutrients, and doing so typically requires movement against a concentration gradient, also known as active transport. So-called primary active transporters derive the energy for such processes from ATP hydrolysis or from light conversion. ATP hydrolysis is catalyzed by protein domains residing outside the membrane that are tightly coupled to the membrane-spanning domain through which the substrate passes.

Many primary transporters also serve as ion pumps; that is, they accumulate, for example,  $H^+$  or  $Na^+$  ions on one side of the membrane and thereby generate an electrochemical gradient. Such concentration gradients are used as an energy source by membrane proteins known as secondary active transporters. Specifically, these proteins power the movement of one substrate against its gradient by harnessing the energy released from the dissipation of the gradient of a different substrate. The transport process may involve the substrates moving either in the same (symport) direction or the opposite (antiport) direction. In all cases, these transporters function according to so-called alternating-access mechanisms (67), whereby the binding sites for the substrates are alternately exposed to one side of the membrane or the other, but not to both at the same time (reviewed in, for example, Reference 43).

## Membrane Enzymes

Many enzymatic reactions carried out by water-soluble proteins are also conducted by enzymes that are integrally embedded in the membrane. The membrane setting facilitates access to hydrophobic substrates such as TM helices destined for proteolysis, but it must also allow access to reactive water molecules. Recent structural studies have shown that membrane enzymes achieve this feat by means of different strategies. For example, the TM helices of UbiA prenyltransferases surround a central hydrophilic active site cavity that is accessible to hydrophobic substrates from the membrane via a hydrophobic tunnel (62). In contrast, the trimeric enzyme diacylglycerol kinase A (DgkA), which phosphorylates lipid headgroups, forms three distinct active sites at the height of the lipid-water interface on the outer surface of the enzyme (86). Perhaps the most unexpected strategy is the aqueous microenvironment within the hydrophobic region of the lipid bilayer created by an exposed hydrophilic patch on the outer surface of membrane proteases. This patch is thought to be the active site for proteolysis (reviewed in References 35, 160).

## Cofactor Scaffolding Proteins

The orientational confinement imposed by the lipid bilayer can also hold a functional advantage. During photosynthesis, for example, light is absorbed by cofactors in so-called light-harvesting

#### Oligomers:

assemblies of two or more protein chains with either the same sequence (homooligomers) or different sequences (heterooligomers)

#### Symmetric proteins:

proteins that are composed of identical sequences replicated around a symmetry axis, which are therefore invariably homooligomeric complexes

complexes (LHCs) and, by way of resonance energy transfer, activates neighboring photosynthetic reaction centers (PRCs). By fixing the relative positions of their cofactors at a specific distance apart, LHCs and PRCs create optimal conditions for light absorption and transfer. Similarly, electron-transfer reactions in the membranes of mitochondria and respiratory bacteria are facilitated by a series of scaffolding proteins known as complexes I to IV, which serve to fix the positions of various iron-containing redox centers. Ultimately, both photosynthesis and respiration result in an  $H^+$  or  $Na^+$  electrochemical gradient across the membrane, which is harnessed by a significantly more dynamic membrane motor protein called ATP synthase (also known as complex V) to energize the production of ATP. See, for example, Reference 155 for a review of these processes.

## FUNCTIONAL DIVERSITY, PROTEIN SIZE, AND SYMMETRY

The assortment of functions described above appears to require a very diverse array of protein architectures. A possible evolutionary strategy to achieve this diversity is to create larger proteins and complexes from smaller structural units (50, 85). This strategy likely has a number of advantages: creation of new protein surfaces capable of binding to different molecules; enhanced stability, for example, by shielding of hydrophobic surfaces that are narrower than the membrane width (10, 116); conformational stability of multimeric complexes; and the potential to support cooperative or other regulatory mechanisms, for example, by tethering distinct functions within heterooligomers. As I explain below, larger proteins are created either by the assembly of multiple subunits, or by the fusion of duplicated or dissimilar genes; symmetry appears to be an intrinsic consequence of both of these processes (50, 85).

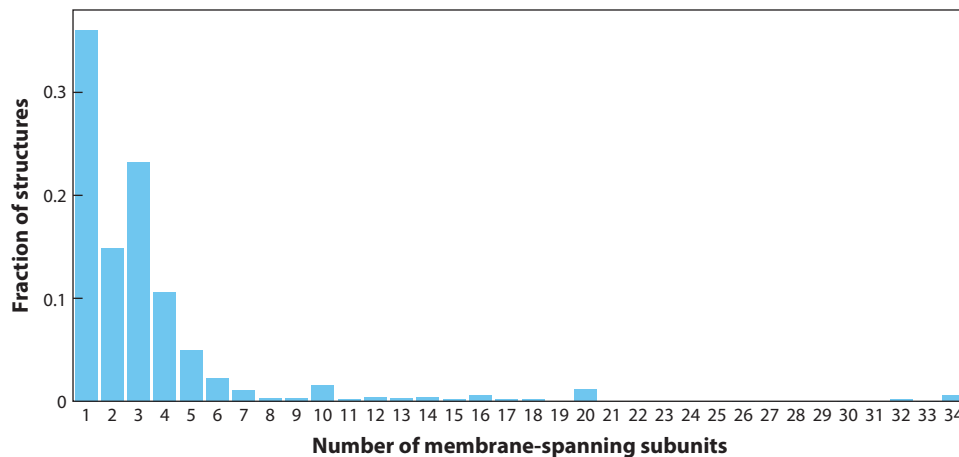
### Oligomerization

The simplest mechanism by which larger proteins are formed is through assembly into homooligomers or heterooligomers. Oligomerization is remarkably common; Levy et al. (85) showed that between one-half and two-thirds of all proteins form obligate complexes. Unfortunately, the equivalent numbers for membrane protein structures have not been well documented, although a cursory analysis of the Protein Data Bank of Transmembrane Proteins (PDBTM) (151) suggests that a similarly large fraction of membrane proteins (~65%) are obligate oligomers; that is, they have more than one membrane-spanning subunit (85) (see **Figure 1**).

Symmetry is found in ~85% of protein complexes and is therefore the norm (85). It has been proposed that symmetry arises naturally from the fact that symmetric protein-protein interfaces contain duplications of all pairwise contacts. Thus, the most favorable interactions are also duplicated, leading to more stable interfaces than those achievable by nonsymmetric complexes (4, 100). A simple survey of available structures (as in the section titled “Symmetry in Membrane Protein Structures”; see **Tables 1–3** and **Figure 2**) suggests that membrane protein oligomers are also predominantly symmetric, although a systematic statistical analysis would be desirable. It will also be important to assess whether the above arguments regarding interface energies also apply within the context of the hydrophobic membrane environment, as well as whether the reduced degrees of freedom in the membrane either enhance or diminish this inherent predisposition toward symmetry.

### Gene Fusion

A second solution to the need for larger and/or more complex proteins is to combine preexisting domains by gene fusion (50). Indeed, the majority of all proteins (55–67%) contain multiple detectable subdomains (107). When considering only membrane proteins, however, the tendency



**Figure 1**

Degree of oligomer formation in membrane protein structures, shown as the fraction of structures that contain one or more membrane-spanning subunits. Data were taken from the Protein Data Bank of Transmembrane Proteins (PDBTM) database (151) dated August 1, 2014, which contains 2,241 proteins. No filtering to remove low-resolution or redundant models was applied. Thus, each data point may contain several representatives from the same structural family. This analysis is necessarily biased toward proteins that crystallize and that are well studied (108). The oligomers are formed via interactions between membrane domains and/or between fused water-soluble domains.

is reversed: only approximately 30% of these proteins contain multiple, independently functioning TM domains (93). Notably, this lack of fusion between membrane protein domains is not due to an inherent inability of their genes to fuse: Indeed, as many as 90% of membrane proteins contain water-soluble domains (93). Thus, it may be that the reduced dimensionality of the membrane enhances the stability of protein–protein interactions, reducing the need for gene fusion of the membrane domains (93).

If fusion of membrane-spanning segments is indeed less common than fusion of water-soluble domains, then one must assume that more complicated membrane protein functions, such as cooperativity, occur preferentially via oligomerization. However, the fraction of membrane protein oligomers in PDBTM (**Figure 1**) is similar to that found for all proteins (85). A more systematic analysis of available membrane protein structures may help to resolve this apparent discrepancy.

## Internal Repeats

The discussion above pertains to the fusion of domains with independent functionality. However, larger proteins can also be constructed by fusion of genes encoding small protein segments; for example, fusion may occur after duplication of secondary structure elements (102), which results in internal structural repeats. Of the proteins containing detectable internal repeats, roughly half are symmetric, suggesting that these proteins originated from concurrent duplication and fusion of genes that encoded homooligomeric complexes (1). In other cases, duplication and subsequent fusion of segments that did not previously form oligomers may have resulted in nonsymmetric internal repeats (1). In either case, after fusion, internal repeat sequences are independently exposed to selective point mutations. Thus, in the absence of a specific functional reason to maintain perfect internal symmetry, the primary sequences of the repeats are very likely to diverge, resulting in structures that are internally pseudosymmetric rather than symmetric (108).

**Internal repeats:** duplications of a structural element or sequence motif within a single polypeptide chain

**Table 1** Membrane proteins of known structure with nonsymmetrical or twofold symmetrical architectures

Order	None	Twofold					
Axis		Perpendicular		Planar			Dihedral
Group		C <sub>2</sub>	pC <sub>2</sub>	C <sub>2</sub>	pC <sub>2</sub>	2 <sub>2</sub>	pD <sub>2</sub>
Receptor, enzyme	OST (95), Proteases (88), TatC (135), YidC (82)	AMPAR (142), <b>Class C GPCR</b> (79), <b>Complex III</b> (163), <b>Complex IV</b> (64), <b>Glycophorin A</b> (103), <b>PS-II</b> (155), Rhodanese (34), RTK (83)	Complex II (147), DsbB (63), NMDAR (73), PRC (27), Rhodopsin (21), UbiA (62),				
Primary transporter	P-type ATPase (149)	ABC export (25), ABC import I (60), ABC import II (97), <b>SR-II</b> (51)	ABC export (2), ABC import I (124), BR (21)		<i>ABC import II*</i> (97)		
Secondary transporter		CDF (99), SemiSWEET (164), <b>APC</b> (36), <b>CLC</b> (31), <b>DASS</b> (106), <b>EIIC</b> (17)	MATE (54), SWEET (65), <b>RND*</b> (33)	<b>SMR</b> (41, 152)	<b>CLC*</b> (31), <b>APC*</b> (45), <i>CaCA</i> (89), <i>CNT*</i> (69), <i>DASS*</i> (106), <i>EAAT*</i> (22), <i>NCS2</i> (98), <i>NPAI*</i> (140)	Mrp* (32)	<i>MFS</i> (58)
Channel	BcsA (117)	MgtE (53), <b>SKT</b> (16), <b>CLC</b> (31)		Gramicidin A (6)	Amt (76), FNT* (157), MIP* (114), SecY (153), TMBIM (18), UT (84)		

Protein families (or one subunit of a larger complex) are organized by symmetry order, axis orientation (perpendicular or parallel to the membrane), and symmetry group. Citations are for structures, analyses thereof, or reviews describing each family. pC<sub>2</sub> indicates a pseudo-C<sub>2</sub> symmetry axis. Bold text indicates a possible regulatory role (e.g., stability, cooperativity). Blue text indicates asymmetry. Italic text indicates that the corresponding symmetry axis runs through the helices of the two repeats (interdigitating repeats). Asterisks indicate listed symmetry is found within a protomer in an oligomeric complex. pD<sub>n</sub> indicates *n*-fold dihedral pseudosymmetry. Protein names, abbreviations, and, in some cases, functions are as follows: ABC, ATP binding cassette; AMPAR, α-amino-3-hydroxy-5-methyl-4-isoxazolepropionic acid receptor; Amt, ammonia channels; APC, amino acid/polyamine/organocation superfamily, which includes the Na<sup>+</sup>-coupled amino acid transporter LeuT, and the betaine/carnitine/choline transporter (BCCT) families; BcsA, subunit A of the cellulose synthesis and translocation system; BR, bacteriorhodopsin, a light-driven H<sup>+</sup> pump; CaCA, Ca<sup>2+</sup>/cation antiporter family; CDF, cation diffusion facilitator; CLC, Cl<sup>−</sup> channel family, which includes Cl<sup>−</sup>/H<sup>+</sup> antiporters; CNT, concentrative nucleoside transporter; complex II, succinate:ubiquinone reductase; complex III, cytochrome *b*<sub>L</sub>; complex IV, cytochrome *c* oxidase aa<sub>3</sub>; DASS, divalent anion:Na<sup>+</sup> symporter; DsbB, disulfide bond formation protein B, a thiol oxidase responsible for disulfide bond formation in *Escherichia coli*; EAAT, excitatory amino acid transporter; EIIC, subunit C of the phosphoenolpyruvate-carbohydrate phosphotransferase transport system; FNT, formate/nitrite transporter; GPCR, G protein-coupled receptor; MATE, multidrug and toxin extrusion transporter; MFS, major facilitator superfamily, which exhibits a hitherto unappreciated twofold dihedral symmetry; MgtE, Mg<sup>2+</sup> channels; MIP, major intrinsic proteins; Mrp, Na<sup>+</sup>/H<sup>+</sup> antiporter related to the transport domains in complex I of the respiratory chain; NCS2, nucleobase:cation symporter-2; NMDAR, N-methyl-D-aspartate receptor; NPAI, Na<sup>+</sup>/H<sup>+</sup> antiporter I; OST, oligosaccharyl transferase; PRC, photosynthetic reaction center; rhodanese is a thiosulfate-cyanide sulfurtransferase; RND, resistance-nodulation-division transporter; RTK, receptor tyrosine kinase; SecY, protein-conducting channel; SKT, superfamily of K<sup>+</sup> transporters; SMR, small multidrug resistance; SR-II, sensory rhodopsin II, a light-driven ion pump that forms a dimer through its transducer protein (HtrII); SWEET, sugar transporters of the SWEET (monomer), SemiSWEET (heterodimer), and Pnu (monomer) families; TatC, twin-arginine protein transport component; TMBIM, transmembrane Bax inhibitor motif family; UbiA, prenyl-transferase family; UT, urea transporter; YidC, Sec-independent membrane protein insertion chaperone.

**Table 2** Membrane proteins of known structure with threefold or fourfold symmetrical architectures

Order	Threefold		Fourfold		
Group	$C_3$	$pC_3$	$C_4$	$pC_4$	$D_4$
Receptor, enzyme	DgkA (86), MAPEG (40), plant LHC2 (94), pMMO (90)	Complex IV (64), NOR (57), pMMO* (90)			
Primary transporter		M-PPase (75)			
Secondary transporter	<b>BCCT</b> (133), <b>RND</b> (120), <b>CNT</b> (69), <b>EAAT</b> (167)	MCP (128)			
Channel	CTR (26), DEG-eNaC (68), Dermcidin (143), P2XR (74), RND (30), <b>Amt</b> (76), <b>OMP</b> (139), <b>SLAC</b> (19), <b>UT</b> (84)	DEG-eNaC (68), UreI* (146)	AMPAR <sup>†</sup> (142), KcsA (29), M2 (61), Nav (127), <b>MIP</b> (114)	NMDAR <sup>†</sup> (73), SKT (16),	AQP-0 (49)

Protein families (or one subunit of a larger complex) are organized by symmetry order and symmetry group. Citations are for structures, analyses thereof, or reviews describing each family.  $D_n$  indicates  $n$ -fold dihedral symmetry;  $pC_n$  indicates a pseudo- $C_n$  symmetry axis. Bold text indicates a possible regulatory role (e.g., stability, cooperativity). Blue text indicates asymmetry. Asterisks indicate listed symmetry is found within a protomer in an oligomeric complex. Daggers indicate mixed symmetry:  $C_4$  symmetry applies only in the channel region, whereas the entire complex has an overall twofold symmetry or pseudosymmetry. Protein names, abbreviations, and, in some cases, functions are as follows: Amt, ammonia channels; AMPAR,  $\alpha$ -amino-3-hydroxy-5-methyl-4-isoxazolepropionic acid-subtype glutamate receptor; AQP-0, aquaporin-0, an MIP-family member; BCCT, betaine/choline/carnitine transporters, which belong to the amino acid/polyamine/organocation (APC) superfamily, and therefore also exhibit  $pC_2$  symmetry (see **Table 1**); BR, bacterial rhodopsin family of light-driven  $H^+$  pumps; Complex IV, cytochrome  $c$  oxidase; CNT, concentrative nucleoside transporters; CTR, copper uptake proteins; DEG-eNaC, degenerin epithelial sodium channel family, including acid-sensing ion channels (ASICs), which can form both homomeric and heteromeric channels; DgkA, diacylglycerol kinase A; EAAT, excitatory amino acid transporter; KcsA,  $K^+$  channel from *Streptomyces lividans*; M2, influenza virus M2 proton-selective ion channel; MAPEG, membrane-associated proteins in eicosanoid and glutathione mechanism; MCP, mitochondrial carrier protein; MIP, major intrinsic protein superfamily, which includes the aquaporin family of proteins; M-PPase, membrane pyrophosphatase; Nav, voltage-gated sodium channel; NMDAR,  $N$ -methyl-D-aspartate subtype glutamate receptor; NOR, nitric oxide reductase; P2XR, P2X receptor channel; plant LHC2, plant light-harvesting complex II; pMMO, particulate methane monooxygenase; OMP, outer-membrane  $\beta$ -barrel protein; RND, resistance-nodulation-division transporter, with a channel component in the outer membrane; SKT, superfamily of  $K^+$  transporters; SLAC, slow anion channel; UreI, proton-gated inner-membrane urea channel; UT, urea transporter.

The first studies of internal structural pseudosymmetry in membrane proteins suggested that the proportion of available membrane protein structures containing pseudosymmetry is as high as one-half (21, 55), although a recent study using a more conservative repeat-detection strategy identified pseudosymmetry in only  $\sim 24\%$  of membrane protein structures (121). The discrepancy between these studies suggests that a quarter of membrane proteins may contain highly divergent internal repeats that are difficult to detect, although the possibility that recently reported structures are less pseudosymmetric remains. Regardless of the exact frequency, given that the proportion of all folds found to be internally pseudosymmetric was  $\sim 18\%$ , available membrane protein structures are clearly enriched in internal pseudosymmetry compared with water-soluble proteins (121).

For a few membrane protein families, hints of these internal structural duplications were identified based on sequence analyses, long before structures were available (see, for example, References 125, 137). However, many other duplications were too distantly related ( $<10\%$  identity) to be detected by such methods (21, 55, 77, 121).

**Pseudosymmetric proteins:** two or more protein segments with differing sequences but shared topological arrangements (folds) of their backbones



**Table 3** Membrane proteins of known structure with fivefold or higher symmetrical architectures

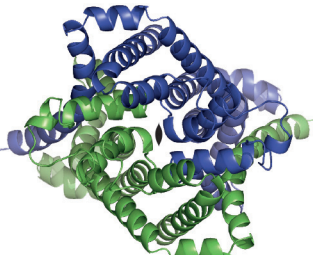
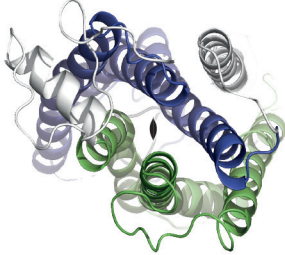
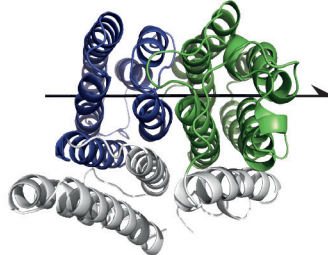
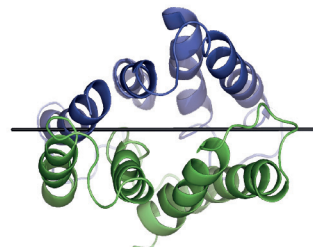
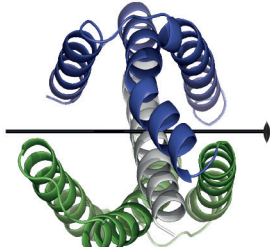
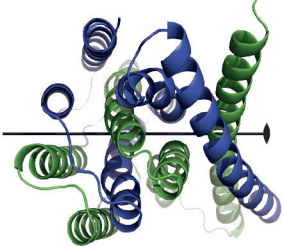
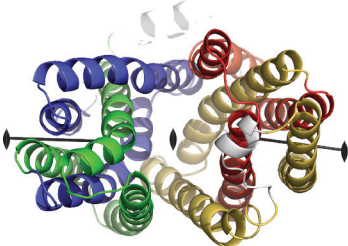
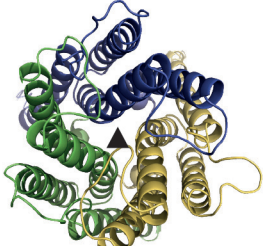
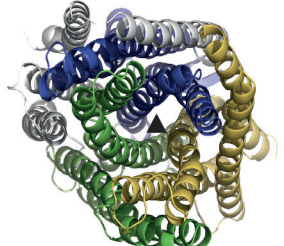

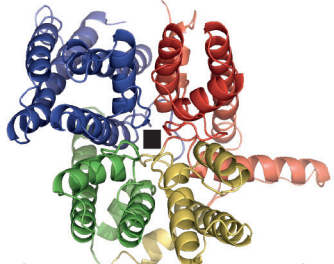
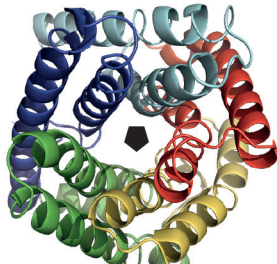
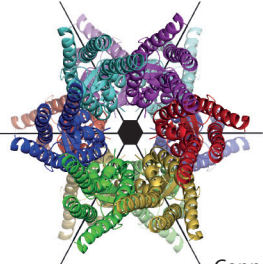
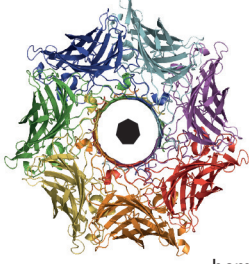
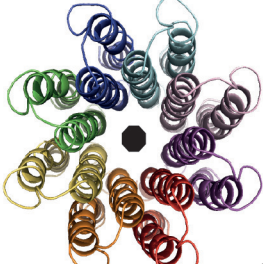
Order	Fivefold		Sixfold		Sevenfold	Eightfold or higher
Group	C <sub>5</sub>	pC <sub>5</sub>	C <sub>6</sub>	D <sub>6</sub>	C <sub>7</sub>	C <sub>8+</sub> or pC <sub>8+</sub>
Receptor, enzyme						Bacterial LH2 [C <sub>8-9</sub> ] (112), LH1 [C <sub>16</sub> ] (122)
Primary transporter						F/V/A-ATPase c-rings* [C <sub>8</sub> , C <sub>10</sub> -C <sub>15</sub> , and pC <sub>11</sub> ] (110)
Secondary transporter						
Channel	pLGICs (56), CorA (101), <b>FNT</b> (157)	Bestrophin (166), pLGIC (115), SLAC* (19)	MARVEL (7), <b>UreI</b> (146)	Cx (104)	MscS (9), CDC (130)	Cytolysin [C <sub>12</sub> ] (119), OMA [C <sub>8</sub> ] (28), OMP [pC <sub>8</sub> -pC <sub>24</sub> ] (37)

Protein families (or one subunit of a larger complex) are organized by symmetry order and symmetry group. Citations are for structures, analyses thereof, or reviews describing each family. pC<sub>n</sub> indicates a pseudo-C<sub>n</sub> symmetry axis; D<sub>n</sub> indicates n-fold dihedral symmetry. Higher-order symmetry groups are given in brackets. Bold text indicates a proposed regulatory role (e.g., stability, cooperativity). Asterisks indicate listed symmetry is found within a larger oligomeric complex. Protein names, abbreviations, and, in some cases, functions, are as follows: CDC, cholesterol-dependent cytolysin pore-forming toxin; CorA, Mg<sup>2+</sup> channel family; Cx, connexin; Cytolysin, α-helical pore-forming toxin; FNT, formate/nitrite transporter; LH1, light-harvesting complex (LHC)-1; bacterial LH2, bacterial LHC-2; MARVEL, myelin and lymphocyte (MAL) and related proteins for vesicle trafficking and membrane link family; MscS, small mechanosensitive channel; OMA, outer-membrane auxiliary proteins, including the Wza polysaccharide translocon; OMP, outer-membrane β-barrel protein; pLGIC, pentameric ligand-gated ion channels, or Cys-loop receptors, which include homomeric receptors, as in the bacterial ELIC channel, and heteromeric complexes such as the nicotinic acetylcholine receptor; SLAC, slow anion channel; UreI, proton-gated inner membrane urea channel.

**Figure 2**

Types of point symmetry in membrane protein structures. Structures are shown as cartoon helices, viewed down onto the membrane. Colored segments indicate symmetric elements, such as independent chains or internal repeats (indicated by asterisks); nonsymmetric elements are shown in gray. Labels in the lower left corner of each box indicate the symmetry or pseudosymmetry type for that structure. ModB<sub>2</sub> (PDB ID: 2ONK), from the homodimeric molybdate type I ATP binding cassette (ABC) importer has twofold symmetry (60), and rhodopsin has twofold pseudosymmetry (21); in both cases, the symmetry axis runs perpendicular to the membrane. Pseudosymmetry about a twofold (2<sub>2</sub>) screw axis parallel to the membrane plane is seen only in the Mrp antiporter-like subunits of complex I (Nqo14; see **Figure 4**). EmrE (PDB ID: 3B5D) is an asymmetric homodimer in its antiparallel form (20). BsYetJ (PDB ID: 4PGW) is a pH-dependent Ca<sup>2+</sup> channel from the transmembrane (TM) Bax inhibitor motif (TMBIM) family and contains a pseudosymmetric inverted repeat; the closed form is shown (18). NCX cation antiporters (PDB ID: 3V5U) contain asymmetric inverted repeats and are therefore both asymmetric and pseudosymmetric (89). The symmetry axis in EmrE, NCX, BsYetJ, and Nqo14 lies parallel to the membrane. Fucose permease (PDB ID: 3O7Q) is a major facilitator superfamily (MFS) member (23). The MFS fold contains twofold C<sub>2</sub> pseudosymmetry axes, one perpendicular to and another parallel to the membrane plane, and it therefore exhibits dihedral D<sub>2</sub> pseudosymmetry; the approximately coincident axes of the six-TM helix N- and C-terminal domains are shown independently. The outward open form of fucose permease shown is also asymmetric (131). Human five-lipoxygenase activating protein (FLAP) (PDB ID: 2Q7M) is an enzyme belonging to the family of membrane-associated proteins involved in eicosanoid and glutathione metabolism (MAPEG), and has threefold C<sub>3</sub> symmetry (40). M-PPase (PDB ID: 4AV3) is a Na<sup>+</sup>-pumping membrane pyrophosphatase from *Thermatoga maritima* with threefold pseudosymmetry (75). Nav is a tetrameric voltage-gated Na<sup>+</sup> channel from *Arcobacter butzleri* (PDB ID: 3RVZ) with fourfold rotational symmetry (127). TrkH (PDB ID: 3PJZ) is a K<sup>+</sup> channel from the superfamily of K<sup>+</sup> transporters (SKT) with fourfold pseudosymmetry (16). In both Nav and TrkH, the cation pore follows the symmetry axis. TehA (PDB ID: 3M73, chain A) is a pentameric slow anion channel (SLAC) homolog with fivefold rotational symmetry (19). Connexin26 (PDB ID: 2ZW3) is a gap junction; each hexameric hemichannel exhibits C<sub>6</sub> symmetry, and each hemichannel spans one membrane, leading to an overall dihedral symmetry (104). α-Hemolysin (PDB ID: 7AHL) is a toxin that assembles to form a C<sub>7</sub>-symmetric pore (144). The F-type ATP synthase membrane rotor c-ring (PDB ID: 2XND) shows C<sub>8</sub> (or higher) symmetry (159). Symmetry axes were defined using SymD v1.3 (78), and figures were made with PyMOL v1.7 (Schrödinger LLC; <http://www.pymol.org>).



 <p><math>C_2</math> ModB2</p>	 <p>Pseudo-<math>C_2</math> Rhodopsin</p>	 <p>Pseudo-<math>2_2</math> screw* Nqo14</p>
 <p><math>C_2</math>, asymmetric EmrE</p>	 <p>Pseudo-<math>C_2^*</math> BsYetJ</p>	 <p>Pseudo-<math>C_2^*</math>, asymmetric NCX</p>
 <p><math>pD_2^*</math>, asymmetric Fucose permease</p>	 <p><math>C_3</math> FLAP</p>	 <p>Pseudo-<math>C_3</math> M-PPase</p>
 <p><math>C_4</math> Nav</p>	 <p>Pseudo-<math>C_4^*</math> TrkH</p>	 <p><math>C_5</math> TehA</p>
 <p><math>D_6</math> Connexin26</p>	 <p><math>C_7</math> α-hemolysin</p>	 <p><math>C_{8+}</math> c-ring</p>

### Nonsymmetric

**proteins:** proteins that neither show any apparent symmetry-related internal duplications nor any symmetry relationship between chains in a multisubunit complex

### Dihedral symmetry with order $N$ :

proteins exhibiting this symmetry contain  $2 \times N$  units related by  $N$  twofold rotational axes and one  $N$ -fold rotational axis

## SYMMETRY IN MEMBRANE PROTEIN STRUCTURES

Lipid bilayers contain a planar symmetry that divides the hydrophobic core in half and reflects the two leaflets. One might therefore expect that some membrane proteins contain a similar structural symmetry, namely, one about an axis running along the midplane of the membrane. Nevertheless, one should keep in mind that the chemical environments on the two sides of the membrane typically are not equivalent.

### Nonsymmetric Membrane Proteins

By definition, the  $\sim 35\%$  of soluble and membrane proteins that are monomeric (50, 85) (**Figure 1**) cannot adopt oligomeric symmetry. Moreover, 57–82% of individual domains also contain no internal repeats (21, 121) and therefore also lack any detectable symmetry. Such nonsymmetric proteins ought to be well suited to detecting differences between the environments on each side of the membrane (50). Indeed, no class of receptor with known structures, namely GPCRs, ligand-gated ion channels, and enzyme-linked receptors such as RTKs, exhibits any apparent symmetry with respect to the membrane plane. Nevertheless, proteins belonging to all these families feature structural symmetry around an axis perpendicular to the membrane (see the subsection titled “Symmetry with the axis perpendicular to the membrane plane”).

Enzymatic reactions in the membrane appear to be accomplished readily by nonsymmetric architectures. These include oligosaccharide transferase (OST) (95), aspartate proteases (88), site-2-proteases (38), and rhomboid proteases (158, 162) (**Table 1**). Nonsymmetric folds are also found in the protein translocation systems YidC (82) and TatC (135), as well as in a cellulose synthesis and translocation system, the BcsA/BcsB complex (117). In the latter case, the eight TM helices of BcsA are organized into pairs, but they are not related by symmetry. Finally, the P-type ATPases, which constitute one of the largest families of primary transporters (149), are clearly nonsymmetric (**Table 1**). Such a lack of symmetry is unusual among transport proteins.

Given that  $\sim 35\%$  of membrane proteins are monomeric (**Figure 1**), one might expect the list of nonsymmetric proteins given in **Table 1** to be significantly longer. Perhaps the monomeric proteins instead contain internal symmetry. It has been estimated that as many as  $\sim 25$ –50% of domains contain no internal pseudosymmetry and therefore should be listed as nonsymmetric in **Table 1** (21, 121); it is possible that the automated approaches used in those studies underestimate the occurrence of internal repeats because the evolutionary divergence of these repeats makes their relationships difficult to detect (1, 121). As a telling example, most GPCRs have been classified as nonsymmetric (121), even though rhodopsin (a GPCR) contains a clear structural duplication of three transmembrane (TM) helices (21). Thus, the repeats in GPCRs seem to have diverged significantly. An effective strategy for identifying symmetry in these structures might therefore be to assign pseudosymmetry to a given structural class based on an analysis of all known structures in that class, rather than using representative folds.

### Cyclic Symmetry

When surveying the most common symmetry groups in oligomeric structures, Levy et al. (85) found that 80% of oligomers contained dihedral symmetry, whereas only 20% were cyclic. In contrast, internally duplicated segments are  $>90\%$  rotationally symmetric (121). A survey of available symmetries in membrane proteins (both internal and oligomeric; see **Tables 1–3** and **Figure 2**) corroborates previous observations that membrane proteins differ from water-soluble proteins in that the vast majority of membrane protein symmetries are cyclic (21, 121), even for oligomers. Indeed, only a few cases with dihedral symmetry were found (see the subsection titled

“Dihedral and Plane Symmetries”). In contrast, almost all imaginable cyclic symmetry groups are found in the available membrane protein structures (**Figure 2**).

**Symmetry with the axis perpendicular to the membrane plane.** The majority of symmetric membrane proteins contain a rotational symmetry about an axis that runs perpendicular to the membrane plane (**Figure 2**). This type of symmetry axis implies that the N-terminal and C-terminal ends of all involved chains are located on the same side of the membrane, presumably simplifying the insertion process.

**Take your partner by the hand: cyclic twofold ( $C_2$ ) symmetry and pseudosymmetry with a perpendicular axis.** The simplest symmetric arrangement, and among the most common in membrane proteins, involves a 180° rotation around an axis perpendicular to the membrane ( $C_2$ , **Table 1**). As described below, ideal  $C_2$  symmetry is found in homooligomeric complexes, whereas  $C_2$  pseudosymmetry is observed both within heterooligomeric complexes and between internal repeats (**Figure 2**). In cases in which this association is known to be required for function, the symmetric elements almost always create a binding site or pathway at their interface (**Table 1**).

Signaling receptors such as RTKs, for example, create a ligand binding site at the dimer interface (83, 87). Each protomer contains extracellular and intracellular domains that are connected by a single TM helix. Binding of the ligand to the extracellular domains causes dimerization or triggers a conformational change within a preexisting dimer (83). Recent structures obtained by NMR of isolated TM helix homodimers, for example, ErbB2 (11), and heterodimers, for example, ErbB1/ErbB2 (113), are consistent with  $C_2$  symmetry or pseudosymmetry extending into the membrane.

Primary transporters of the ATP binding cassette (ABC) transporter family assemble using  $C_2$  perpendicular symmetry, creating both a substrate pathway and ATP binding sites at the dimer interface (132). All ABC transporters contain two TM domains (TMDs) and two ABCs (also known as nucleotide binding domains, NBDs), which are assembled either from separate chains or from fused domains. Notably, the NBDs create two off-axis binding sites for ATP using a head-to-tail arrangement, whereas the substrate pathway typically follows the symmetry axis.

Four different classes of ABC transporters have been identified (96): ABC exporters and three types of ABC importers, called type I, type II, and energy coupling factor (ECF) importers. Simple homodimers are found in three of these classes, for example, forming local  $C_2$  symmetry in the TM domains of the type I importer ModB<sub>2</sub> (60) (**Figure 2**) and in those of the type II importer BtuC<sub>2</sub> (97). Heterodimeric ABC transporters, in contrast, come together in pseudo- $C_2$ -symmetric complexes, as exemplified by MalF and MalG, which form the TM segments of the ABC importer MalFGK (124). In some cases, one NBD has lost the ability to hydrolyze ATP. A structure of an ABC exporter with one of these so-called degenerate NBDs contains a nucleotide bound to only one site, creating an asymmetry in these soluble domains (59); such asymmetry has intriguing functional implications (as reviewed in, for example, Reference 147).

Perpendicular pseudo- $C_2$ -symmetry is also seen in some secondary transporters (**Table 1**; **Figures 2** and **3**), notably in the largest class, the major facilitator superfamily (MFS) (126). Structural studies confirmed that the MFS fold contains two lobes of six TM helices, each lining a central pathway (58). Interestingly, the multidrug and toxin extrusion (MATE) transporters, such as NorM (54), and the resistance-nodulation-division (RND) transporters, exemplified by AcrB (33), also contain two domains of six TM helices lining a central pathway. Nevertheless, the topological arrangements of the helices differ between these three folds.

Beyond the aforementioned functional roles, dimerization of membrane proteins also appears to be a common strategy for regulation (**Table 1**), for example, by enhancing stability or

---

**Protomer:**

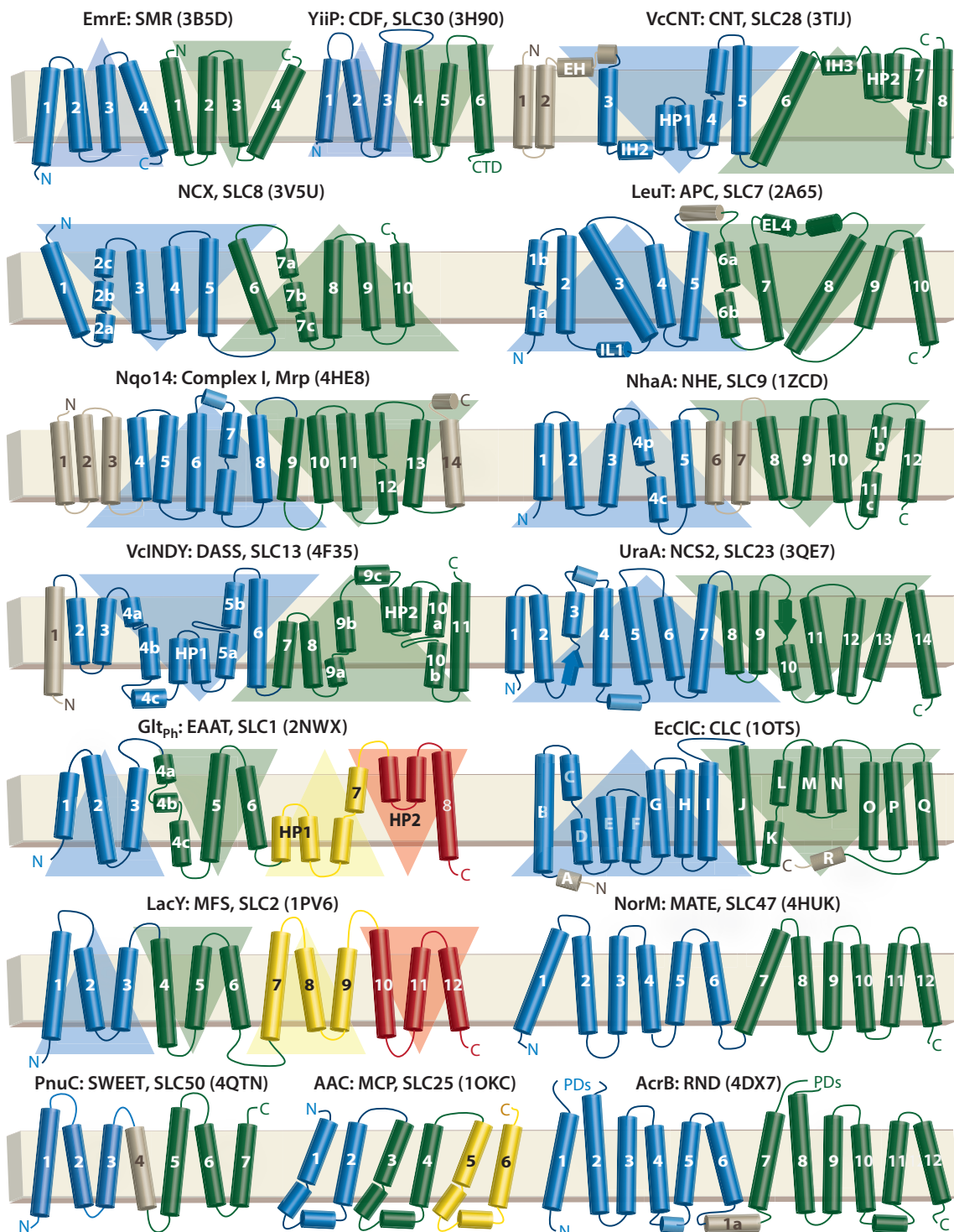
a single subunit of a homooligomeric subunit, as distinct from a monomer, which is a nonoligomeric entity

**Asymmetric**

**proteins:** protein segments with similar folds that adopt distinct conformations of their backbones within the context of the same fold

---





introducing allostery. Dimerization of class C GPCRs allows them unique modes of activation (79). By extension, the occurrence and functional relevance of homooligomerization and heterooligomerization by class A GPCRs is the focus of intense study (39).

**Threefold symmetry is often found in regulatory roles.** As mentioned in the subsection titled “Membrane Enzymes,” the trimeric enzyme DgkA is proposed to form active sites at the interface between adjacent protomers in a threefold symmetric arrangement (**Table 2**). The positioning of these sites on the exterior of the protein at the level of the lipid headgroups provides access for both hydrophobic (diacylglycerol) and hydrophilic (ATP) substrates (86). Homotrimeric assemblies also create channels and pathways. Examples include the P2X ATP-gated ion channels (74) and the outer membrane protein component of the RND efflux systems called TolC (30). Membrane proteins with diverse functions are assembled from triplicated internal repeats with pseudo- $C_3$  symmetry (**Table 2**). In the ion-pumping pyrophosphatases (M-PPases) (**Figure 2**) (75, 91) and mitochondrial carrier proteins (MCPs) (**Figure 3**) (128), for example, these repeats surround the central substrate binding sites and/or pathways.

Strikingly, no perfectly threefold-symmetric structures have been reported for transporters, at least not for their core transport units (**Table 2**). Homotrimeric assemblies of secondary transporters and channels are common, however, apparently for regulatory reasons. For example, trimerization of the  $\text{Na}^+$ -coupled aspartate transporter Glt<sub>Ph</sub>, a homolog of the excitatory amino acid transporters (EAATs), may help stabilize the protein within the membrane during its large, elevator-like conformational change (22, 134).

Interestingly, asymmetry between protomers is also seen in trimeric transporter assemblies such as the RND transporter AcrB (120) (**Table 2**). Furthermore, within each protomer of AcrB, two parallel repeats (**Table 1**; **Figure 3**) cycle through three distinct conformational states, resulting in  $\text{H}^+$  uptake (33). These changes in the membrane domains are mechanically transduced to a periplasmic domain; this domain also cycles through three distinct states, resulting in drug extrusion. The asymmetry in the trimer results from coupling of the transport cycles of the three protomers, owing to an extensive interface between the periplasmic domains. This asymmetric coupling mechanism may minimize the extent of drug backflow (33). Interactions involving the cytoplasmic tails of neighboring protomers (133) also lead to an asymmetry in the trimeric  $\text{Na}^+$ -coupled betaine transporter, BetP (150), possibly providing a mechanism for the increase in its transport rate in response to osmotic stress (138).

## Figure 3

Transmembrane topologies of secondary transporters with known structure. The outside of the cell or organelle is oriented to the top. Protein name, family name, and human solute carrier (SLC) nomenclature, if applicable, are given for each protein, and representative PDB IDs are given in parentheses. Helices are represented as cylinders, and strands are represented as arrows. Each inverted-topology repeat is highlighted using a triangle; the bases of these triangles indicate the side of the N terminus for each segment. The cation diffusion facilitator (CDF) dimerizes through contacts between C-terminal domains (CTDs). The PnuC protein includes an additional N-terminal TM helix (not shown) that is not conserved among SWEET transporters; semiSWEET transporters (e.g. 164) resemble a dimer of TM1–3 and TM4–6 of the vitamin B<sub>3</sub> transporter, PnuC, but with a domain swap (66). Nqo14 is a subunit of the NADH:oxidoreductase complex I, related to the Mrp family cation exchangers; see **Figure 4** for more details. Abbreviations: AAC, ADP–ATP carrier; APC, amino acid/polyamine/organocation superfamily; CLC,  $\text{Cl}^-$  channels/antiporters; CNT, concentrative nucleoside transporter; DASS, divalent anion: $\text{Na}^+$  symporter; EAAT, excitatory amino acid transporter; MATE, multidrug and toxin extruder protein; MCP, mitochondrial carrier protein; MFS, major facilitator superfamily; NCS2, nucleobase cation symporter-2; NCX,  $\text{Na}^+/\text{Ca}^{2+}$  cation exchanger; NHE,  $\text{Na}^+/\text{H}^+$  exchanger; RND, resistance-nodulation-division transporter; PDs, periplasmic domains; SMR, small multidrug resistance; SWEET, sugar transporter; Vc, *Vibrio cholera*; YiiP,  $\text{H}^+$ -coupled  $\text{Zn}^{2+}$  transporter from *Escherichia coli*.

**Mixed symmetries:**  
 the presence of two or  
 more distinct  
 symmetry  
 relationships within  
 the context of a  
 multidomain complex

**Higher cyclic symmetries in channels and other systems.** The creation of a central pathway is a common feature of parallel membrane protein oligomers (**Figure 2**), resulting in hollow rings with between 3-fold and 12-fold symmetry (**Tables 2 and 3**). Tetramers include  $K^+$  and  $Na^+$  channels such as the voltage-gated  $Na^+$  channel NavAb (127) (**Figure 2**), the M2  $H^+$  channel from influenza A virus (61), and the channel regions of ionotropic glutamate receptors (iGluRs) such as the AMPA-subtype receptor (142). Many channels are pentameric, e.g., the anion channel TehA from the plant slow anion channel (SLAC) family (19) (**Figure 2**), although hexamers, such as a MARVEL [myelin and lymphocyte (MAL) and related proteins for vesicle trafficking and membrane link family]-domain channel called synaptophysin (7); heptamers, such as the small mechanosensitive channel, MscS (9); and octamers, as in the outer membrane polysaccharide translocon Wza (28), have all been observed. The largest pore-forming oligomers are constructed from toxins such as the cytolysins (130) (**Table 3**), using both  $\alpha$ -helical and  $\beta$ -barrel TM segments (155). Indeed, a toxin called perfringolysin O may create a pore-forming complex with 40–50 protomers; such a complex would undoubtedly represent the highest cyclic symmetry order in a membrane protein (130, 141).

Rings of membrane proteins perform roles other than pore formation (**Table 3**). For example, LHCs form ovals or rings to transfer the light energy harnessed during photosynthesis to PRCs located in the center of the complex (**Table 3**) (112, 122). Another example is the rotor ring of the F-type ATP synthases. The rotor rings are likely to be plugged by lipids (129) and facilitate  $H^+$  or  $Na^+$  permeation at their outer surface as they rotate against an adjacent static subunit (71, 129). Because three ATP molecules are synthesized for every revolution of the ring, the number of subunits in the rotor ring (which in most cases equals the number of transported ions) determines the thermodynamic capacity of the enzyme to synthesize ATP (109).

Pseudosymmetry is less common in  $\alpha$ -helical complexes of higher order (**Tables 2 and 3**, **Figure 2**), although some channels are composed of repeated elements (e.g. TrkH; see Reference 16), and other channels and receptors are known to form heteromers (e.g., heterotetrameric NMDA-subtype iGluRs, which are formed of dimers of heterodimers; see Reference 73), as do some of the membrane rings of rotary ATPase enzymes (109). In contrast, in outer-membrane  $\beta$ -barrel proteins (OMPs), the  $\beta$ -strands typically belong to a continuous polypeptide chain and are related by an 8-fold to 24-fold rotational pseudosymmetry (37) (**Table 3**).

**Mixed symmetries.** In some heteromeric membrane protein complexes it is possible to identify subdomains whose symmetries vary. In these cases, the membrane domain often exhibits a higher symmetry order than that of the extramembrane domains. Examples include the ATP synthases and ATPases, which have membrane rotor rings that adopt  $C_8$  or higher symmetry or pseudosymmetry (see the subsection titled “Higher cyclic symmetries in channels and other systems”) and which are connected by so-called stalk segments to a large catalytic domain that comprises a trimer of heterodimers related by  $C_6$  pseudosymmetry (as reviewed in, for example, Reference 71).

As mentioned in the subsection titled “Higher cyclic symmetries in channels and other systems,” the channel regions of iGluRs have fourfold rotational symmetry (in AMPA-subtype receptors; see Reference 142) or pseudosymmetry (in NMDA-subtype receptors; see Reference 73). Remarkably, however, the same protein chains that form the channel extend into extracellular domains that have only twofold symmetry (or pseudosymmetry) because the domains are arranged as pairs of local dimers (73, 111, 142). Thus, iGluRs exhibit mixed symmetries within the same protein chain.

**The membrane-bisecting axis of rotation.** The discovery in recent years of multiple examples of rotational symmetries about axes that run along a plane bisecting the membrane has been a surprising one (**Figure 2**). Prior to these findings, the only example of such a protein was a unique

bacterial channel-forming antibiotic called gramicidin A, which is composed of D-amino-acids that cause it to form a  $\beta$ -helix (14). Gramicidin A is too short to span the entire lipid bilayer and so forms head-to-head dimers related by a planar  $C_2$  symmetry axis, thereby satisfying its hydrogen-bonding potential within the hydrophobic membrane core (6). For typical  $\alpha$ -helical transmembrane helices, however, the membrane-bisecting axis of rotation raises energetic conundrums because the protein must either (a) insert nonhelical segments deep into the bilayer and risk exposing polar groups to the hydrophobic core or (b) insert the entire protein with dual TM topologies, seemingly a challenge for the insertion machinery. Such issues of membrane protein folding are reviewed in Reference 12.

Most of the membrane-bisecting  $C_2$  symmetries relate internal repeats with an odd number of TM helices (**Figure 2**). As a result, the topologies of these repeats are inverted with respect to one another, placing their N termini on opposite sides of the membrane (**Figure 3, Table 1**) and resulting in  $C_2$  pseudosymmetry. The only characterized dimers whose protomers are related by a symmetry axis oriented in this way are the small multidrug resistance (SMR) transporters (**Figures 2 and 3**) and the FluC fluoride channel (145).

An underappreciated distinction emerges when comparing inverted-topology folds, namely the orientation of the membrane-bisecting symmetry axis relative to the repeats. The symmetry axis may lie in between the two repeats of a protein, in which case each repeat has an independent fold (see the EmrE structure in **Figure 2**), or the axis may pass through the center of both repeats, in which case the helices of the two repeats must interdigitate (see the NCX and fucose permease structures in **Figure 2**).

**Adjacent inverted-topology repeats.** Interestingly, inverted-repeat folds in which the repeats are adjacent to the axis of symmetry are found mostly in channels (**Table 1**). Many of these channels are specific for small polar molecules such as water (aquaporin 1, Aqp1; Reference 114), urea (*Desulfovibrio vulgaris* urea transporter, dvUT; Reference 84), or ammonia (AmtB; Reference 76). In addition, adjacent inverted-topology repeats are found in channels and transporters for small anions (e.g., CLC family transporters and channels) (31) and for cations, as in the Bax inhibitor homolog, BsYetJ (**Figure 2**) (18). Unusually, the two three-TM helix repeats in BsYetJ surround the seventh TM helix, through which the pseudosymmetry axis also passes (**Figure 2**).

With the exception of BsYetJ, the interface between adjacent repeats typically defines two symmetry-equivalent pathways that lead from either side of the membrane to the center of the protein (44). This strategy for channel formation seems to be evolutionarily parsimonious because a single duplication leads to a narrow pathway that is well suited to conducting small molecules (145).

**Interdigitating inverted-topology repeats.** Proteins that contain interdigitating inverted-topology structural repeats have arguably the most complex of the known membrane protein folds (**Figure 3**), and these proteins are mainly involved in secondary transport (italicized elements in **Table 1**). However, interlocking repeat elements also contribute to subdomains in larger transporters; for example, in type II ABC importers, four TM helices within each lobe contribute to a pseudosymmetric inverted repeat (21, 97). Similarly, each twofold symmetric lobe in the MFS fold is itself composed of interdigitating three-TM helix inverted-topology repeats (58), leading to an overall twofold dihedral pseudosymmetry (**Figures 2 and 3**). As a result, the MFS fold can be considered to contain interlocking inverted-topology repeats of six TM helices (131). As described in the subsection titled “Asymmetry in membrane proteins,” a functional advantage of such interlocking inverted-topology repeats may be an ability to adopt asymmetric states that fulfill the requirements for alternating access.

---

**Topology:** the direction of threading of protein segments back and forth across the membrane

**Dual-topology:** the ability of a protein to insert into the membrane in both orientations with equal probability; also known as undecided or frustrated topology

**Inverted-topology repeats:** membrane protein segments in a single chain inserted in opposite orientations, and related by a twofold axis running parallel to the membrane

---



**Domain swapping:** the positional exchange of one or more secondary structure elements from neighboring protomers in an oligomeric complex

Interdigitation leads to wide spacing between contiguous helices (in sequence), implying that the isolated repeats are unlikely to be well folded. The resulting interfaces between interlocked helices are indistinguishable in nature from those in the interior of proteins (50), namely, they have minimal hydration and extensive hydrophobic cores, in stark contrast to the interfaces of typical oligomers. The folding of interdigitated proteins must therefore be a complex process, particularly in the context of the membrane, and it would be interesting to examine whether individual inverted-topology repeats can exist as independently folded units.

The possible evolutionary origins of such a complex fold are also enigmatic. However, their interfaces are reminiscent of those in domain-swapping water-soluble proteins (92), and this similarity may provide a useful starting point for further inquiry.

**Asymmetry in membrane proteins.** Although symmetric and pseudosymmetric arrangements predominate, many membrane proteins exhibit a structural asymmetry that is essential for function (blue elements in **Tables 1** and **2**). Asymmetry in a homooligomer has the evolutionary handicap that the asymmetric interface must evolve to optimize interactions with two different environments simultaneously (50). This disadvantage may explain the rarity of such interfaces, but functional advantages appear in some cases to compensate that energetic cost.

The first example of functional asymmetry in membrane proteins was provided by the homodimeric SMR transporter EmrE (20, 41, 152). In structures of EmrE, the two identical protein chains adopt an antiparallel orientation with different conformations and, as a result, create a pathway to one side of the membrane only (**Figure 2**). This fold is an example of classical asymmetry. Around the same time, a distinctive asymmetry was also found to underlie the formation of the outward-facing state of an amino acid transporter, LeuT (44, 45). The asymmetry in LeuT was obscured by the pseudosymmetry of the repeats (165), which contain <10% identical residues and therefore also exhibit some level of inherent structural divergence. Once detected, however, the asymmetry could be taken advantage of, and used to model an alternate state. Specifically, each repeat was used as a template for homology modeling of the other repeat, so that each repeat adopts the other conformation. In this way, by threading the sequence of the first repeat onto the structure of the second repeat, and vice versa, the two halves of the protein swap conformations. This conformation swapping strategy applied to LeuT resulted in a model of an inward-facing state (45), the general features of which are remarkably consistent with a structure determined subsequently (80).

These findings imply that, by creating an asymmetry between the two repeats, proteins such as EmrE and LeuT can adopt two states, consistent with an alternating-access cycle (i.e., with pathways leading to one side of the membrane or the other). Thus, to transition to the other major conformation in the transport cycle, the protein undergoes asymmetry exchange, wherein the first repeat (or protomer) adopts the conformation of the second repeat (or protomer), and vice versa (41, 45), resulting in a new asymmetric structure that is open to the other side of the membrane. Given that substrate accumulation in physiological contexts is driven only by the balance of substrate concentrations and the associated membrane potentials, all conformations of the transporter must be similarly accessible from an energetic standpoint, without any additional input (unlike primary transporters, for which a direct energy input is required). The degeneracy of structural states implied by the asymmetry-exchange mechanism described above is an elegant solution to this requirement.

The repeat-swapping strategy for modeling the structures of alternate states of asymmetric transporters has since been applied to proteins with diverse structural folds (**Figure 3**), including the aspartate transporter Glt<sub>Ph</sub> (22), the Na<sup>+</sup>/Ca<sup>2+</sup> exchanger (NCX) from the Ca<sup>2+</sup>:cation exchanger family (CaCA) (89), lactose permease from the MFS (131), and NhaA from the Na<sup>+</sup>:H<sup>+</sup>

antiporter (NPA) family (140). Notably, all of these folds comprise inverted repeats with interdigitating helices (italicized elements in **Table 1**, **Figure 2**). A model of an alternate state was generated for each of these cases, and the predicted global conformational changes were later validated by structures (42, 43, 134, 156) or other biophysical and biochemical evidence (131, 140). Importantly, NMR spectroscopy data support the proposal that antiparallel EmrE functions by exchanging between degenerate states (118). Thus, the asymmetry-exchange mechanism underlies alternating access by both homodimers and pseudosymmetric interdigitating inverted repeats.

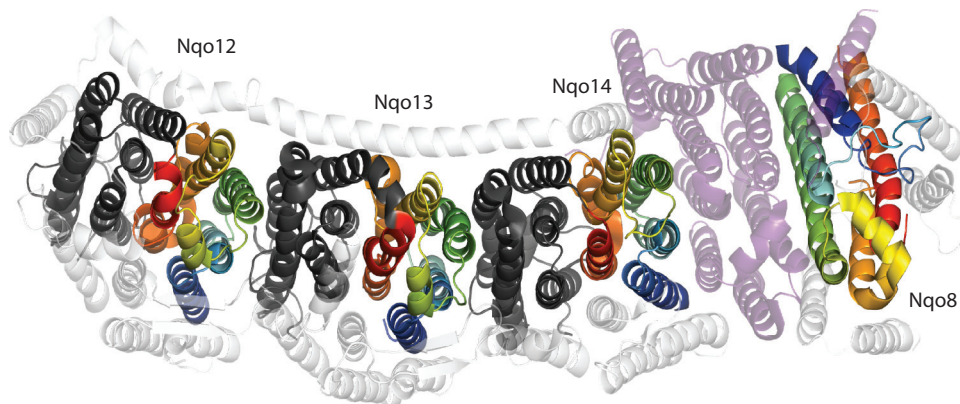
How do asymmetric transporters optimize their substrate pathways to interact equally favorably with two different environments (50), that is, to both achieve protein–protein packing and interact with substrate and/or aqueous solution? In Glt<sub>ph</sub>, these interfaces comprise smooth surfaces with both polar and hydrophobic character (134), which is likely to reduce the probability of the protein becoming trapped in one state.

A notable conundrum posed by the asymmetry-exchange mechanism is the role of symmetric states. Let us consider two subunits, A and B, both of which can adopt two conformations, *i* and *j*. The asymmetric states of the transporter can thus be defined as A<sub>*i*</sub>B<sub>*j*</sub> or A<sub>*j*</sub>B<sub>*i*</sub>. What prevents the formation of A<sub>*i*</sub>B<sub>*i*</sub> or A<sub>*j*</sub>B<sub>*j*</sub>? Might one of these arrangements correspond to an occluded state or, possibly, to a leaky state (105)?

Intriguingly, asymmetry has recently been detected in the antiparallel homodimeric F<sup>−</sup> channel, FluC (C. Miller, personal communication), although the reason why a channel requires asymmetry is unclear. Still, pure asymmetry such as that found in EmrE and FluC is rare, and the inverted repeats of asymmetry-exchanging transporters typically have divergent sequences. Pseudosymmetry may therefore play an important role in adapting secondary transporters to diverse substrates and conditions. In some cases, the breakdown in symmetry may also reduce the free energy of one state over the other just enough to provide preferential conformations of the transporter, for example, while awaiting substrate binding. Analysis of putative common ancestors of asymmetry-exchanging transporters may therefore provide useful insights into the minimal requirements for secondary transport.

Note that in principle, it is possible to achieve such diversity and conformational bias using heterodimeric proteins rather than fused internal repeats. As heterodimers are relatively rare among secondary transporters, fusing two domains into a single larger protein may have additional advantages, for example, in terms of stability or folding within the membrane.

**Face-to-back inverted-topology repeats.** Remarkably, a pseudosymmetry involving a screw axis with a membrane-bisecting axis was recently identified within a membrane protein subunit related to Na<sup>+</sup>/H<sup>+</sup> antiporters of the Mrp family (32) (**Table 1**, **Figure 2**). Specifically, the multimeric NADH:ubiquinone oxidoreductase, or complex I of the respiratory chain, was demonstrated to contain a five-TM helix internal repeat within each of three subunits (Nqo12, Nqo13, and Nqo14) responsible for H<sup>+</sup> pumping (**Figure 4**). Because they are related by a pseudotwofold screw axis (2<sub>2</sub>) rather than a rotational axis (C<sub>2</sub>), however, the repeats are oriented face-to-back, rather than adjacent or interdigitating (32). An additional domain (Nqo8), which also contains one of these repeat units, is located close to the NADH:ubiquinone electron transfer site (8). This structure shows how the screw axis is well suited to creating a linear (in effect, helical) array of subunits with repeated interactions. The repeated arrangement presumably facilitates multiple simultaneous pathway openings and closures in response to electron transfer at one end of the complex. The interfaces between repeats in Nqo14 and Nqo13, for example, are similar to those between repeats within each subunit (**Figure 4**). Molecular dynamics simulation studies indicate that the formation of aqueous proton channels that open alternately to either side of the membrane may require



**Figure 4**

The membrane domain of complex I from *Thermus thermophilus* (8) (PDB ID: 4HE8) viewed from the periplasm. Inverted-topology repeats related by a twofold ( $2_2$ ) screw axis are colored blue to red for the first repeat unit or dark gray for the second repeat unit. The single repeat unit in the Nqo8 subunit has the same transmembrane topology as the first repeat units in the other three domains, but this domain is more tilted than Nqo12, Nqo13, and Nqo14 are, and it is rotated by  $180^\circ$  around an axis perpendicular to the membrane plane (cf. *dark blue helices*). Nqo8 is separated from Nqo14 by several additional subunits (*purple*). Other nonsymmetric segments and subunits are shown in white.

exchange between symmetry-related states (72), similar to the asymmetry-exchange mechanism described above in the subsection titled “Asymmetry in membrane proteins.”

## Dihedral and Plane Symmetries

Dihedral and planar symmetries contain within them a twofold symmetry axis and are therefore in principle compatible with membranes. In dihedral symmetry, however, there must be rotational twofold axes both perpendicular to and parallel to the membrane plane (154). Thus, dihedral symmetry within a protein spanning a single membrane potentially exposes polar groups to the hydrophobic membrane core. One possible solution is found in protein complexes that span two membranes. For example, in gap junctions, two hemichannels, one per membrane, are stacked up to create a pore across the two membranes. Each hemichannel is formed by a hexamer of connexin proteins with  $C_6$  symmetry, and the entire gap junction exhibits a dihedral ( $D_6$ ) symmetry (104) (Table 3, Figure 2). Similarly, in the lens of the eye, aquaporin-0 (AQP-0) tetramers pack head-to-head into octamers that span the membranes of the lens fiber cells, creating a  $D_4$  dihedral symmetry (Table 2) (49).

Dihedral symmetry can also be achieved by interchelating the repeated elements. MFS transporters, which have a dimer of inverted repeats, satisfy this requirement. As mentioned in the subsection titled “Interdigitating inverted-topology repeats,” these proteins have a twofold pseudosymmetry axis perpendicular to the membrane that relates the six-TM helix halves, combined with a twofold pseudosymmetry axis parallel to the membrane that relates two interchelated three-TM helix repeats in each half (Figures 2 and 3). Thus, MFS transporters contain  $D_2$  dihedral pseudosymmetry (Table 2) while maintaining the unsatisfied hydrogen bond potential in the aqueous solution away from the hydrophobic membrane core.

Although they are rare, plane symmetries, which are created by translations in two directions, are found in arrays of membrane proteins at specific cellular structures. These include ribbons of claudin proteins at epithelial tight junctions (46, 148) and arrays of AQP-0 octamers (15). Both

specific and nonspecific properties of the lipids may be critical for the formation of such arrays (24, 48).

## Higher-Order Cubic and Space-Group Symmetries

The planar nature of lipid membranes renders the three-dimensional arrangements associated with higher-order cubic or space-group symmetries unavailable to membrane proteins. However, attachments to scaffolding or anchoring proteins may result in the formation of spatially ordered complexes by assemblies of membrane proteins.

## Dynamic Transitions Between Symmetry Types

Many membrane proteins function via dynamic conformational changes. The example of secondary transporters described in the subsection titled “The membrane-bisecting axis of rotation” illustrates how such a functional conformational cycle can involve a transition between two low-energy asymmetric states. Other proteins may require transitions from symmetric to asymmetric states or transitions from one type of symmetry to another. Channel gating and/or activation can involve asymmetric intermediates or progressive, stepwise conformational changes of independent subunits. For example, the closed channel form of the Bax inhibitor homolog BsYetJ is pseudosymmetric (**Figure 2**), but the open form is asymmetric, owing to a movement of a single TM helix (18). In voltage-gated cation channels, each pore-lining subunit is connected to a voltage-sensing domain (see the Nav structure in **Figure 2**) for which voltage-induced movements are transmitted to the channel-lining helices to increase the probability that the helices adopt an open conformation. For example, it has been shown that during activation of the tetrameric *Shaker* K<sup>+</sup> channel, the gating in each subunit is independent, and therefore the complex must visit asymmetric intermediate conformations (168). However, the combined activation of all four subunits is required to form a new, symmetric, open state of the channel.

The subunits in iGluRs can also be activated independently by ligand binding, leading to intermediate conductance states (136). Nevertheless, the complete activation event appears to involve a transition in the extracellular domains from one twofold pseudosymmetric arrangement to a distinct arrangement that is also twofold pseudosymmetric (111). Conformational changes associated with the channel becoming desensitized to its ligand, in contrast, involve a transition to a fourfold-symmetric state in those same extracellular domains. Remarkably, throughout all of these changes in the extracellular domains, the TM channel in iGluRs apparently retains an overall fourfold pseudosymmetry (111).

### SUMMARY POINTS

1. Membrane protein structures to date exhibit a wide range of symmetries and pseudosymmetries from twofold to planar arrays, including mixtures of symmetries within a larger complex, but most conform to cyclic point-group symmetry.
2. The fraction of oligomers in available membrane protein structures is apparently similar to that of water-soluble proteins, but membrane protein structures contain a higher proportion of internal repeats. Overall, membrane proteins may exhibit symmetry more frequently than water-soluble proteins do.
3. Inverted-topology (pseudo)symmetries create channels and pathways through the membrane.

4. Asymmetry has been observed in secondary transporters and in one channel; the majority of these proteins have folds comprising inverted-topology repeats or protomers, both interdigitated and adjacent.
5. Both identical (homooligomeric) and divergent (pseudosymmetric internal repeat) protein sequences use asymmetry-exchange mechanisms to create degenerate alternate states consistent with alternating-access transport mechanisms.
6. Conformational changes in membrane proteins can involve transitions between different symmetry types.

## FUTURE ISSUES

1. Systematic analysis of the growing number of membrane protein structures will be needed to further classify symmetries, pseudosymmetries, oligomerization, and internal repeats in membrane proteins. Continued efforts in structural biology, particularly in noncrystallographic methods such as cryo-electron microscopy will be needed to fill in gaps in fold space.
2. Which factors govern asymmetry in secondary transporters, and how is the balance of asymmetric states affected by substrate binding? How do these factors change for different transporter architectures, and how are they affected by individual point mutations? What is the advantage of fused repeats over small dimeric proteins?
3. Do symmetric (or pseudosymmetric) states play a role in secondary transport by asymmetry-exchange mechanisms, for example, as occluded/closed or leak states?
4. What factors define the boundary between channel and transporter functions (with symmetric and asymmetric functional states, respectively), especially in folds such as the CLCs?
5. What was the evolutionary pathway of inverted-topology interlocking repeats? Are the individual repeats stable as separate entities? Bioinformatic and folding studies of the simplest cases, such as NCX, may help identify contributions from, for example, circular permutation or domain swapping.
6. Did all inverted-topology folds arise from divergent evolution of a single ancestor, or did they arise as a result of convergent evolution from many dual-topology proteins?

## DISCLOSURE STATEMENT

The author is not aware of any affiliations, memberships, funding, or financial holdings that might be perceived as affecting the objectivity of this review.

## ACKNOWLEDGMENTS

Thanks to Jos Faraldo-Gmez for helpful discussions, suggestions and comments on the manuscript. This work was supported by the Intramural Research Program of the National Institutes of Health, National Institute of Neurological Disorders and Stroke.



## LITERATURE CITED

1. Abraham A-L, Pothier J, Rocha EPC. 2009. Alternative to homo-oligomerisation: the creation of local symmetry in proteins by internal amplification. *J. Mol. Biol.* 394(3):522-34
2. Aller SG, Yu J, Ward A, Weng Y, Chittaboina S, et al. 2009. Structure of P-glycoprotein reveals a molecular basis for poly-specific drug binding. *Science* 323(5922):1718-22
3. Alm  n MS, Nordstr  m KJV, Fredriksson R, Schi  th HB. 2009. Mapping the human membrane proteome: a majority of the human membrane proteins can be classified according to function and evolutionary origin. *BMC Biol.* 7(1):50
4. Andr   I, Strauss CEM, Kaplan DB, Bradley P, Baker D. 2008. Emergence of symmetry in homooligomeric biological assemblies. *PNAS* 105(42):16148-52
5. Arabidopsis Genome Initiative. 2000. Analysis of the genome sequence of the flowering plant *Arabidopsis thaliana*. *Nature* 408(6814):796-815
6. Arseniev AS, Lomize AL, Barsukov IL, Bystrov VF. 1986. Gramicidin A transmembrane ion-channel. Three-dimensional structure reconstruction based on NMR spectroscopy and energy refinement. *Biol. Membr.* 3(11):1077-104 (from Russian)
7. Arthur CP, Stowell MHB. 2007. Structure of synaptophysin: a hexameric MARVEL-domain channel protein. *Structure* 15(6):707-14
8. Baradaran R, Berrisford JM, Minhas GS, Sazanov LA. 2013. Crystal structure of the entire respiratory complex I. *Nature* 494:443-48
9. Bass RB, Strop P, Barclay M, Rees DC. 2002. Crystal structure of *Escherichia coli* MscS, a voltage-modulated and mechanosensitive channel. *Science* 298(5598):1582-87
10. Benjamini A, Smit B. 2012. Robust driving forces for transmembrane helix packing. *Biophys. J.* 103(6):1227-35
11. Bocharov EV, Mineev KS, Volynsky PE, Ermolyuk YS, Tkach EN, et al. 2008. Spatial structure of the dimeric transmembrane domain of the growth factor receptor ErbB2 presumably corresponding to the receptor active state. *J. Biol. Chem.* 283(11):6950-56
12. Bowie JU. 2013. Structural biology. Membrane protein twists and turns. *Science* 339(6118):398-99
13. Bracey MH, Cravatt BF, Stevens RC. 2004. Structural commonalities among integral membrane enzymes. *FEBS Lett.* 567(2-3):159-65
14. Busath DD. 1993. The use of physical methods in determining gramicidin channel structure and function. *Annu. Rev. Physiol.* 55:473-501
15. Buzhynskyy N, Sens P, Behar-Cohen F, Scheuring S. 2011. Eye lens membrane junctional microdomains: a comparison between healthy and pathological cases. *New J. Phys.* 13(8):085016
16. Cao Y, Jin X, Huang H, Derebe MG, Levin EJ, et al. 2011. Crystal structure of a potassium ion transporter, TrkH. *Nature* 471(7338):336-40
17. Cao Y, Jin X, Levin EJ, Huang H, Zong Y, et al. 2011. Crystal structure of a phosphorylation-coupled saccharide transporter. *Nature* 473(7345):50-54
18. Chang Y, Bruni R, Kloss B, Assur Z, Kloppmann E, et al. 2014. Structural basis for a pH-sensitive calcium leak across membranes. *Science* 344(6188):1131-35
19. Chen Y-H, Hu L, Punta M, Bruni R, Hillerich B, et al. 2010. Homologue structure of the SLAC1 anion channel for closing stomata in leaves. *Nature* 467(7319):1074-80
20. Chen Y-J, Pornillos O, Lieu S, Ma C, Chen AP, Chang G. 2007. X-ray structure of EmrE supports dual topology model. *PNAS* 104(48):18999-19004
21. Choi S, Jeon J, Yang J-S, Kim S. 2008. Common occurrence of internal repeat symmetry in membrane proteins. *Proteins* 71(1):68-80
22. Crisman TJ, Qu S, Kanner BI, Forrest LR. 2009. Inward-facing conformation of glutamate transporters as revealed by their inverted-topology structural repeats. *PNAS* 106(49):20752-7
23. Dang S, Sun L, Huang Y, Lu F, Liu Y, et al. 2010. Structure of a fucose transporter in an outward-open conformation. *Nature* 467(7316):734-38
24. Davies KM, Anselmi C, Wittig I, Faraldo-G  mez JD, K  hlbrandt W. 2012. Structure of the yeast F<sub>1</sub>F<sub>0</sub>-ATP synthase dimer and its role in shaping the mitochondrial cristae. *PNAS* 109:13602-7

---

8. The first structure of a face-to-back inverted-topology repeat.

---



---

12. Insightful overview of membrane protein insertion and folding, particularly important for dual-topology proteins.

---

31. The only known structure of a membrane protein containing inverted-topology repeats.

41. Structural modeling using electron microscopy data for antiparallel EmrE; the authors propose an asymmetry-exchange mechanism.

45. Authors propose asymmetry exchange for pseudosymmetric repeats in LeuT and demonstrate accessibility of proposed pathway.

25. Dawson RJP, Locher KP. 2006. Structure of a bacterial multidrug ABC transporter. *Nature* 443(7108):180–85
26. De Feo CJ, Aller SG, Siluvai GS, Blackburn NJ, Unger VM. 2009. Three-dimensional structure of the human copper transporter hCTR1. *PNAS* 106(11):4237–42
27. Deisenhofer J, Epp O, Miki K, Huber R, Michel H. 1985. Structure of the protein subunits in the photosynthetic reaction centre of *Rhodospseudomonas viridis* at 3 Å resolution. *Nature* 318(6047):618–24
28. Dong C, Beis K, Nesper J, Brunkan-LaMontagne AL, Clarke BR, et al. 2006. Wza the translocon for *E. coli* capsular polysaccharides defines a new class of membrane protein. *Nature* 444(7116):226–29
29. Doyle DA, Morais Cabral J, Pfuetzner RA, Kuo A, Gulbis JM, et al. 1998. The structure of the potassium channel: molecular basis of K<sup>+</sup> conduction and selectivity. *Science* 280(5360):69–77
30. Du D, Wang Z, James NR, Voss JE, Klimont E, et al. 2014. Structure of the AcrAB–TolC multidrug efflux pump. *Nature* 509(7501):512–15
31. Dutzler R, Campbell EB, Cadene M, Chait BT, MacKinnon R. 2002. X-ray structure of a ClC chloride channel at 3.0 Å reveals the molecular basis of anion selectivity. *Nature* 415(6869):287–94
32. Efremov RG, Sazanov LA. 2011. Structure of the membrane domain of respiratory complex I. *Nature* 476(7361):414–20
33. Eicher T, Seeger MA, Anselmi C, Zhou W, Brandstätter L, et al. 2014. Coupling of remote alternating-access transport mechanisms for protons and substrates in the multidrug efflux pump AcrB. *eLIFE* 3:e03145
34. Eichmann C, Tzitzilonis C, Bordignon E, Maslennikov I, Choe S, et al. 2014. Solution NMR structure and functional analysis of the integral membrane protein YgaP from *Escherichia coli*. *J. Biol. Chem.* 289(34):23482–503
35. Erez E, Fass D, Bibi E. 2009. How intramembrane proteases bury hydrolytic reactions in the membrane. *Nature* 459(7245):371–78
36. Fang Y, Jayaram H, Shane T, Kolmakova-Partensky L, Wu F, et al. 2009. Structure of a prokaryotic virtual proton pump at 3.2 Å resolution. *Nature* 460(7258):1040–43
37. Fairman JW, Noinaj N, Buchanan SK. 2011. The structural biology of β-barrel membrane proteins: a summary of recent reports. *Curr. Opin. Struct. Biol.* 21(4):523–31
38. Feng L, Yan H, Wu Z, Yan N, Wang Z, et al. 2007. Structure of a site-2 protease family intramembrane metalloprotease. *Science* 318(5856):1608–12
39. Ferre S, Casado V, Devi LA, Filizola M, Jockers R, et al. 2014. G protein–coupled receptor oligomerization revisited: functional and pharmacological perspectives. *Pharmacol. Rev.* 66(2):413–34
40. Ferguson AD, McKeever BM, Xu S, Wisniewski D, Miller DK, et al. 2007. Crystal structure of inhibitor-bound human 5-lipoxygenase-activating protein. *Science* 317(5837):510–12
41. Fleishman SJ, Harrington SE, Enosh A, Halperin D, Tate CG, Ben-Tal N. 2006. Quasi-symmetry in the cryo-EM structure of EmrE provides the key to modeling its transmembrane domain. *J. Mol. Biol.* 364(1):54–67
42. Forrest LR. 2013. Structural biology. (Pseudo-)symmetrical transport. *Science* 339(6118):399–401
43. Forrest LR, Krämer R, Ziegler C. 2011. The structural basis of secondary active transport mechanisms. *Biochim. Biophys. Acta* 1807(2):167–88
44. Forrest LR, Rudnick G. 2009. The rocking bundle: a mechanism for ion-coupled solute flux by symmetrical transporters. *Physiology* 24:377–86
45. Forrest LR, Zhang Y-W, Jacobs MT, Gesmonde J, Xie L, et al. 2008. Mechanism for alternating access in neurotransmitter transporters. *PNAS* 105(30):10338–43
46. Furuse M, Sasaki H, Fujimoto K, Tsukita S. 1998. A single gene product, claudin-1 or -2, reconstitutes tight junction strands and recruits occludin in fibroblasts. *J. Cell Biol.* 143(2):391–401
47. George AM, Jones PM. 2012. Perspectives on the structure–function of ABC transporters: the Switch and Constant Contact Models. *Prog. Biophys. Mol. Biol.* 109(3):95–107
48. Gonen T, Cheng Y, Sliz P, Hiroaki Y, Fujiyoshi Y, et al. 2005. Lipid–protein interactions in double-layered two-dimensional AQP0 crystals. *Nature* 438(7068):633–38
49. Gonen T, Sliz P, Kistler J, Cheng Y, Walz T. 2004. Aquaporin-0 membrane junctions reveal the structure of a closed water pore. *Nature* 429(6988):193–97



50. Goodsell DS, Olson AJ. 2000. Structural symmetry and protein function. *Annu. Rev. Biophys. Biomol. Struct.* 29:105–53
51. Gordeliy VI, Labahn J, Moukhametziev R, Efremov R, Granzin J, et al. 2002. Molecular basis of transmembrane signalling by sensory rhodopsin II-transducer complex. *Nature* 419(6906):484–87
52. Gross DJ. 1996. The role of symmetry in fundamental physics. *PNAS* 93(25):14256–59
53. Hattori M, Tanaka Y, Fukai S, Ishitani R, Nureki O. 2007. Crystal structure of the MgtE Mg<sup>2+</sup> transporter. *Nature* 448(7157):1072–75
54. He X, Szewczyk P, Karyakin A, Evin M, Hong W-X, et al. 2010. Structure of a cation-bound multidrug and toxic compound extrusion transporter. *Nature* 467(7318):991–94
55. Hennerdal A, Falk J, Lindahl E, Elofsson A. 2010. Internal duplications in  $\alpha$ -helical membrane protein topologies are common but the nonduplicated forms are rare. *Protein Sci.* 19(12):2305–18
56. Hilf RJC, Dutzler R. 2008. X-ray structure of a prokaryotic pentameric ligand-gated ion channel. *Nature* 452(7185):375–79
57. Hino T, Matsumoto Y, Nagano S, Sugimoto H, Fukumori Y, et al. 2010. Structural basis of biological N<sub>2</sub>O generation by bacterial nitric oxide reductase. *Science* 330(6011):1666–70
58. Hirai T, Heymann JAW, Shi D, Sarker R, Maloney PC, Subramaniam S. 2002. Three-dimensional structure of a bacterial oxalate transporter. *Nat. Struct. Biol.* 9(8):597–600
59. Hohl M, Briand C, Gr  t  r MG, Seeger MA. 2012. Crystal structure of a heterodimeric ABC transporter in its inward-facing conformation. *Nat. Struct. Mol. Biol.* 19(4):395–402
60. Hollenstein K, Frei DC, Locher KP. 2007. Structure of an ABC transporter in complex with its binding protein. *Nature* 446(7132):213–16
61. Hong M, DeGrado WF. 2012. Structural basis for proton conduction and inhibition by the influenza M2 protein. *Protein Sci.* 21(11):1620–33
62. Huang H, Levin EJ, Liu S, Bai Y, Lockless SW, Zhou M. 2014. Structure of a membrane-embedded prenyltransferase homologous to UBIAD1. *PLOS Biol.* 12(7):e1001911
63. Inaba K, Murakami S, Suzuki M, Nakagawa A, Yamashita E, et al. 2006. Crystal structure of the DsbB-DsbA complex reveals a mechanism of disulfide bond generation. *Cell* 127(4):789–801
64. Iwata S, Ostermeier C, Ludwig B, Michel H. 1995. Structure at 2.8    resolution of cytochrome c oxidase from *Paracoccus denitrificans*. *Nature* 376(6542):660–69
65. Jaehme M, Guskov A, Slotboom DG. 2014. Crystal structure of the vitamin B<sub>3</sub> transporter PnuC, a full-length SWEET homolog. *Nat. Struct. Mol. Biol.* 21:1013–15
66. Jaehme M, Guskov A, Slotboom DG. 2015. The twisted relation between Pnu and SWEET transporters. *Trends Biochem. Sci.* 40(4):183–88
67. Jardetzky O. 1966. Simple allosteric model for membrane pumps. *Nature* 211(5052):969–70
68. Jasti J, Furukawa H, Gonzales EB, Gouaux E. 2007. Structure of acid-sensing ion channel 1 at 1.9    resolution and low pH. *Nature* 449(7160):316–23
69. Johnson ZL, Cheong C-G, Lee S-Y. 2012. Crystal structure of a concentrative nucleoside transporter from *Vibrio cholerae* at 2.4   . *Nature* 483(7390):489–83
70. Jones CP, Ferr  -D'Amar   AR. 2015. RNA quaternary structure and global symmetry. *Trends Biochem. Sci.* 40(4):211–20
71. Junge W, Lill H, Engelbrecht S. 1997. ATP synthase: an electrochemical transducer with rotatory mechanics. *Trends Biochem. Sci.* 22(11):420–23
72. Kaila VRI, Wikstr  m M, Hummer G. 2014. Electrostatics, hydration, and proton transfer dynamics in the membrane domain of respiratory complex I. *PNAS* 111(19):6988–93
73. Karakas E, Furukawa H. 2014. Crystal structure of a heterotetrameric NMDA receptor ion channel. *Science* 344(6187):992–97
74. Kawate T, Michel JC, Birdsong WT, Gouaux E. 2009. Crystal structure of the ATP-gated P2X<sub>4</sub> ion channel in the closed state. *Nature* 460(7255):592–98
75. Kellosalo J, Kajander T, Kogan K, Pokharel K, Goldman A. 2012. The structure and catalytic cycle of a sodium-pumping pyrophosphatase. *Science* 337(6093):473–76
76. Khademi S, O'Connell J III, Remis J, Robles-Colmenares Y, Miercke LJW, Stroud RM. 2004. Mechanism of ammonia transport by Amt/MEP/Rh: structure of AmtB at 1.35   . *Science* 305(5690):1587–94

---

50. An excellent and comprehensive discussion of symmetry in all classes of proteins.

---

77. Khafizov K, Staritzbichler R, Stamm M, Forrest LR. 2010. A study of the evolution of inverted-topology repeats from LeuT-fold transporters using AlignMe. *Biochemistry* 49(50):10702–13
78. Kim C, Basner J, Lee B. 2010. Detecting internally symmetric protein structures. *BMC Bioinform.* 11(1):303
79. Kniazeff J, Przeau L, Rondard P, Pin J-P, Goudet C. 2011. Dimers and beyond: the functional puzzles of class C GPCRs. *Pharmacol. Ther.* 130(1):9–25
80. Krishnamurthy H, Gouaux E. 2012. X-ray structures of LeuT in substrate-free outward-open and apo inward-open states. *Nature* 481(7382):469–74
81. Krogh A, Larsson B, von Heijne G, Sonnhammer ELL. 2001. Predicting transmembrane protein topology with a hidden Markov model: application to complete genomes. *J. Mol. Biol.* 305(3):567–80
82. Kumazaki K, Chiba S, Takemoto M, Furukawa A, Nishiyama K, et al. 2014. Structural basis of Sec-independent membrane protein insertion by YidC. *Nature* 509(7501):516–20
83. Lemmon MA, Schlessinger J. 2010. Cell signaling by receptor tyrosine kinases. *Cell* 141(7):1117–34
84. Levin EJ, Quick M, Zhou M. 2009. Crystal structure of a bacterial homologue of the kidney urea transporter. *Nature* 462(7274):757–61
85. Levy ED, Pereira-Leal JB, Chothia C, Teichmann SA. 2006. 3D complex: a structural classification of protein complexes. *PLOS Comput. Biol.* 2(11):e155
86. Li D, Lyons JA, Pye VE, Vogeley L, Arago D, et al. 2013. Crystal structure of the integral membrane diacylglycerol kinase. *Nature* 497(7450):521–24
87. Li E, Hristova K. 2010. Receptor tyrosine kinase transmembrane domains: function, dimer structure and dimerization energetics. *Cell Adhes. Migr.* 4(2):249–54
88. Li X, Dang S, Yan C, Gong X, Wang J, Shi Y. 2014. Structure of a presenilin family intramembrane aspartate protease. *Nature* 493(7430):56–61
89. Liao J, Li H, Zeng W, Sauer DB, Belmares R, Jiang Y. 2012. Structural insight into the ion-exchange mechanism of the sodium/calcium exchanger. *Science* 335(6069):686–90
90. Lieberman RL, Rosenzweig AC. 2005. Crystal structure of a membrane-bound metalloenzyme that catalyses the biological oxidation of methane. *Nature* 434(7030):177–82
91. Lin S-M, Tsai J-Y, Hsiao C-D, Huang Y-T, Chiu C-L, et al. 2012. Crystal structure of a membrane-embedded H<sup>+</sup>-translocating pyrophosphatase. *Nature* 484(7394):399–403
92. Liu Y, Eisenberg D. 2002. 3D domain swapping: as domains continue to swap. *Protein Sci.* 11(6):1285–99
93. Liu Y, Gerstein M, Engelman DM. 2004. Transmembrane protein domains rarely use covalent domain recombination as an evolutionary mechanism. *PNAS* 101(10):3495–97
94. Liu Z, Yan H, Wang K, Kuang T, Zhang J, et al. 2004. Crystal structure of spinach major light-harvesting complex at 2.72  resolution. *Nature* 428(6980):287–92
95. Lizak C, Gerber S, Numao S, Aebi M, Locher KP. 2011. X-ray structure of a bacterial oligosaccharyl-transferase. *Nature* 474(7351):350–55
96. Locher KP. 2009. Structure and mechanism of ATP-binding cassette transporters. *Phil. Trans. R. Soc. B.* 364(1514):239–45
97. Locher KP, Lee AT, Rees DC. 2002. The *E. coli* BtuCD structure: a framework for ABC transporter architecture and mechanism. *Science* 296(5570):1091–98
98. Lu F, Li S, Jiang Y, Jiang J, Fan H, et al. 2011. Structure and mechanism of the uracil transporter UraA. *Nature* 472(7342):243–46
99. Lu M, Fu D. 2007. Structure of the zinc transporter YiiP. *Science* 317(5845):1746–48
100. Lukatsky DB, Zeldovich KB, Shakhnovich EI. 2006. Statistically enhanced self-attraction of random patterns. *Phys. Rev. Lett.* 97(17):178101
101. Lunin VV, Dobrovetsky E, Khutoreskaya G, Zhang R, Joachimiak A, et al. 2006. Crystal structure of the CorA Mg<sup>2+</sup> transporter. *Nature* 440(7085):833–37
102. Lynch M, Conery JS. 2000. The evolutionary fate and consequences of duplicate genes. *Science* 290(5494):1151–55
103. MacKenzie KR, Prestegard JH, Engelman DM. 1997. A transmembrane helix dimer: structure and implications. *Science* 276(5309):131–33
104. Maeda S, Nakagawa S, Suga M, Yamashita E, Oshima A, et al. 2009. Structure of the connexin 26 gap junction channel at 3.5  resolution. *Nature* 458:597–602

105. Mager S, Min C, Henry DJ, Chavkin C, Hoffman BJ, et al. 1994. Conducting states of a mammalian serotonin transporter. *Neuron* 12(4):845–59
106. Mancusso R, Gregorio GG, Liu Q, Wang DN. 2012. Structure and mechanism of a bacterial sodium-dependent dicarboxylate transporter. *Nature* 491(7425):622–26
107. Marsden RL, Lee D, Maibaum M, Yeats C, Orengo CA. 2006. Comprehensive genome analysis of 203 genomes provides structural genomics with new insights into protein family space. *Nucleic Acids Res.* 34(3):1066–80
108. Marsh JA, Teichmann SA. 2015. Structure, dynamics, assembly, and evolution of protein complexes. *Annu. Rev. Biochem.* In press. doi: 10.1146/annurev-biochem-060614-034142
109. Matthies D, Zhou W, Klyszejko AL, Anselmi C, Yildiz  , et al. 2014. High-resolution structure and mechanism of an F/V-hybrid rotor ring in a Na<sup>+</sup>-coupled ATP synthase. *Nat. Commun.* 5:5286
110. Meier T, Faraldo-G mez JD, B rsch M. 2011. ATP synthase: a paradigmatic molecular machine. In *Molecular Machines in Biology*, ed. J Frank, pp. 208–38. New York: Cambridge Univ. Press
111. Meyerson JR, Kumar J, Chittori S, Rao P, Pierson J, et al. 2014. Structural mechanism of glutamate receptor activation and desensitization. *Nature* 514(7522):328–34
112. McLuskey K, Roszak AW, Zhu Y, Isaacs NW. 2009. Crystal structures of all-alpha type membrane proteins. *Eur. Biophys. J.* 39(5):723–55
113. Mineev KS, Bocharov EV, Pustovalova YE, Bocharova OV, Chupin VV, Arseniev AS. 2010. Spatial structure of the transmembrane domain heterodimer of ErbB1 and ErbB2 receptor tyrosine kinases. *J. Mol. Biol.* 400(2):231–43
114. Mitsuoka K, Murata K, Walz T, Hirai T, Agre P, et al. 1999. The structure of aquaporin-1 at 4.5-  resolution reveals short  -helices in the center of the monomer. *J. Struct. Biol.* 128(1):34–43
115. Miyazawa A, Fujiyoshi Y, Unwin N. 2003. Structure and gating mechanism of the acetylcholine receptor pore. *Nature* 423(6943):949–55
116. Mondal S, Johnston JM, Wang H, Khelashvili G, Filizola M, Weinstein H. 2013. Membrane driven spatial organization of GPCRs. *Sci. Rep.* 3:2909
117. Morgan JLW, Strumillo J, Zimmer J. 2013. Crystallographic snapshot of cellulose synthesis and membrane translocation. *Nature* 493(7431):181–86
118. Morrison EA, DeKoster GT, Dutta S, Vafabakhsh R, Clarkson MW, et al. 2012. Antiparallel EmrE exports drugs by exchanging between asymmetric structures. *Nature* 481(7379):45–50
119. Mueller M, Grauschopf U, Maier T, Glockshuber R, Ban N. 2009. The structure of a cytolytic  -helical toxin pore reveals its assembly mechanism. *Nature* 459(7247):726–30
120. Murakami S, Nakashima R, Yamashita E, Matsumoto T, Yamaguchi A. 2006. Crystal structures of a multidrug transporter reveal a functionally rotating mechanism. *Nature* 443(7108):173–79
121. Myers-Turnbull D, Bliven SE, Rose PW, Aziz ZK, Youkharibache P, et al. 2014. Systematic detection of internal symmetry in proteins using CE-Symm. *J. Mol. Biol.* 426(11):2255–68
122. Niwa S, Yu L-J, Takeda K, Hirano Y, Kawakami T, et al. 2014. Structure of the LH1–RC complex from *Thermochromatium tepidum* at 3.0  . *Nature* 508(7495):228–32
123. Nugent T, Jones DT. 2009. Transmembrane protein topology prediction using support vector machines. *BMC Bioinform.* 10(1):159
124. Oldham ML, Khare D, Qui cho FA, Davidson AL, Chen J. 2007. Crystal structure of a catalytic intermediate of the maltose transporter. *Nature* 450(7169):515–21
125. Pao GM, Wu L-F, Johnson KD, H fte H, Chrispeels MJ, et al. 1991. Evolution of the MIP family of integral membrane transport proteins. *Mol. Microbiol.* 5(1):33–37
126. Pao SS, Paulsen IT, Saier MH. 1998. Major facilitator superfamily. *Microbiol. Mol. Biol. Rev.* 62(1):1–34
127. Payandeh J, Scheuer T, Zheng N, Catterall, WA. 2011. The crystal structure of a voltage-gated sodium channel. *Nature* 475(7356):353–58
128. Pebay-Peyroula E, Dahout-Gonzalez C, Kahn R, Tr z guet V, Lauquin GJ-M, Brandolin G. 2003. Structure of mitochondrial ADP/ATP carrier in complex with carboxyatractyloside. *Nature* 426(6962):39–44
129. Pogoryelov D, Krah A, Langer JD, Yildiz  , Faraldo-G mez JD, Meier T. 2010. Microscopic rotary mechanism of ion translocation in the F(o) complex of ATP synthases. *Nat. Chem. Biol.* 6(12):891–99

---

121. Recent assessment of internal pseudosymmetry indicating that membrane proteins are enriched in symmetric structural repeats.

---

130. Popoff MR. 2014. Clostridial pore-forming toxins: powerful virulence factors. *Anaerobe* 30:220–38
131. Radestock S, Forrest LR. 2011. The alternating-access mechanism of MFS transporters arises from inverted-topology repeats. *J. Mol. Biol.* 407(5):698–715
132. Rees DC, Johnson E, Lewinson O. 2009. ABC transporters: the power to change. *Nat. Rev. Mol. Cell Biol.* 10(3):218–27
133. Ressler S, van Scheltinga ACT, Vonnrhein C, Ott V, Ziegler C. 2009. Molecular basis of transport and regulation in the Na<sup>+</sup>/betaine symporter BetP. *Nature* 457(7234):47–52
134. Reyes N, Ginter C, Boudker O. 2009. Transport mechanism of a bacterial homologue of glutamate transporters. *Nature* 462(7275):880–85
135. Rollauer SE, Tarry MJ, Graham JE, Jaskelinen M, Jager F, et al. 2012. Structure of the TatC core of the twin-arginine protein transport system. *Nature* 492(7428):210–14
136. Rosenmund C, Stern-Bach Y, Stevens CF. 1998. The tetrameric structure of a glutamate receptor channel. *Science* 280(5369):1596–99
137. Saraste M, Walker JE. 1982. Internal sequence repeats and the path of polypeptide in mitochondrial ADP/ATP translocase. *FEBS Lett.* 144(2):250–54
138. Schiller D, Rubenhagen R, Kramer R, Morbach S. 2004. The C-terminal domain of the betaine carrier BetP of *Corynebacterium glutamicum* is directly involved in sensing K<sup>+</sup> as an osmotic stimulus. *Biochemistry* 43(19):5583–91
139. Schirmer T, Keller TA, Wang YF, Rosenbusch JP. 1995. Structural basis for sugar translocation through maltoporin channels at 3.1  resolution. *Science* 267(5197):512–14
140. Schushan M, Rimon A, Haliloglu T, Forrest LR, Padan E, Ben-Tal N. 2012. A model-structure of a periplasm-facing state of the NhaA antiporter suggests the molecular underpinnings of pH-induced conformational changes. *J. Biol. Chem.* 287(22):18249–61
141. Shepard LA, Shatursky O, Johnson AE, Tweten RK. 2000. The mechanism of pore assembly for a cholesterol-dependent cytolysin: Formation of a large prepore complex precedes the insertion of the transmembrane  $\beta$ -hairpins. *Biochemistry* 39(33):10284–93
142. Sobolevsky AI, Rosconi MP, Gouaux E. 2009. X-ray structure, symmetry and mechanism of an AMPA-subtype glutamate receptor. *Nature* 462(7274):745–56
143. Song C, Weichbrodt C, Salnikov ES, Dynowski M, Forsberg BO, et al. 2013. Crystal structure and functional mechanism of a human antimicrobial membrane channel. *PNAS* 110(12):4586–91
144. Song L, Hobaugh MR, Shustak C, Cheley S, Bayley H, Gouaux JE. 1996. Structure of staphylococcal  $\alpha$ -hemolysin, a heptameric transmembrane pore. *Science* 274(5294):1859–65
145. Stockbridge RB, Robertson JL, Kolmakova-Partensky L, Miller C. 2013. A family of fluoride-specific ion channels with dual-topology architecture. *eLIFE* 2:e01084
146. Strugatsky D, McNulty R, Munson K, Chen C-K, Soltis SM, et al. 2013. Structure of the proton-gated urea channel from the gastric pathogen *Helicobacter pylori*. *Nature* 493(7431):255–58
147. Sun F, Huo X, Zhai Y, Wang A, Xu J, et al. 2005. Crystal structure of mitochondrial respiratory membrane protein complex II. *Cell* 121(7):1043–57
148. Suzuki H, Nishizawa T, Tani K, Yamazaki Y, Tamura A, et al. 2014. Crystal structure of a claudin provides insight into the architecture of tight junctions. *Science* 344:304–7
149. Toyoshima C, Nakasako M, Nomura H, Ogawa H. 2000. Crystal structure of the calcium pump of sarcoplasmic reticulum at 2.6  resolution. *Nature* 405:647–55
150. Tsai C-J, Khafizov K, Hakulinen J, Forrest LR, Kramer R, et al. 2011. Structural asymmetry in a trimeric Na<sup>+</sup>/betaine symporter, BetP, from *Corynebacterium glutamicum*. *J. Mol. Biol.* 407:368–81
151. Tuszny GE, Dosztnyi Z, Simon I. 2005. PDB\_TM: selection and membrane localization of transmembrane proteins in the protein data bank. *Nucleic Acids Res.* 33:D275–78
152. Ubarretxena-Belandia I, Baldwin JM, Schuldiner S, Tate CG. 2003. Three-dimensional structure of the bacterial multidrug transporter EmrE shows it is an asymmetric homodimer. *EMBO J.* 22:6175–81
153. van den Berg B, Clemons WM, Collinson I, Modis Y, Hartmann E, et al. 2004. X-ray structure of a protein-conducting channel. *Nature* 427(6969):36–44
154. Venkatakrishnan AJ, Levy ED, Teichmann SA. 2010. Homomeric protein complexes: evolution and assembly. *Biochem. Soc. Trans.* 38:879–82

155. Vinothkumar KR, Henderson R. 2010. Structures of membrane proteins. *Q. Rev. Biophys.* 43(1):65–158
156. Waight AB, Pedersen BP, Schlessinger A, Bonomi M, Chau BH, et al. 2013. Structural basis for alternating access of a eukaryotic calcium/proton exchanger. *Nature* 499(7456):107–10
157. Wang Y, Huang Y, Wang J, Cheng C, Huang W, et al. 2009. Structure of the formate transporter FocA reveals a pentameric aquaporin-like channel. *Nature* 462(7272):467–72
158. Wang Y, Zhang Y, Ha Y. 2006. Crystal structure of a rhomboid family intramembrane protease. *Nature* 444:179–80
159. Watt IN, Montgomery MG, Runswick MJ, Leslie AG, Walker JE. 2010. Bioenergetic cost of making an adenosine triphosphate molecule in animal mitochondria. *PNAS* 107(39):16823–27
160. White SH. 2006. Rhomboid intramembrane protease structures galore! *Nat. Struct. Mol. Biol.* 13:1049–51
161. White SH, ed. 2015. *Membrane Proteins of Known 3D Structure*, updated Feb. 19. Stephen White Lab. UC Irvine, Irvine, CA. <http://blanco.biomol.uci.edu/mpstruc/>
162. Wu Z, Yan N, Feng L, Oberstein A, Yan H, et al. 2006. Structural analysis of a rhomboid family intramembrane protease reveals a gating mechanism for substrate entry. *Nat. Struct. Mol. Biol.* 13:1084–91
163. Xia D, Yu C-A, Kim H, Xia J-Z, Kachurin AM, et al. 1997. Crystal structure of the cytochrome bc<sub>1</sub> complex from bovine heart mitochondria. *Science* 277(5322):60–66
164. Xu Y, Tao Y, Cheung LS, Fan C, Chen LQ, et al. 2014. Structures of bacterial homologues of SWEET transporters in two distinct conformations. *Nature* 515(7527):448–52
165. Yamashita A, Singh SK, Kawate T, Jin Y, Gouaux E. 2005. Crystal structure of a bacterial homologue of Na<sup>+</sup>/Cl<sup>−</sup>-dependent neurotransmitter transporters. *Nature* 437:215–23
166. Yang T, Liu Q, Kloss B, Bruni R, Kalathur RC, et al. 2014. Structure and selectivity in bestrophin ion channels. *Science* 346(6207):355–59
167. Yernool D, Boudker O, Jin Y, Gouaux E. 2004. Structure of a glutamate transporter homologue from *Pyrococcus horikoshii*. *Nature* 431(7010):811–18
168. Zagotta WN, Hoshi T, Aldrich RW. 1994. Shaker potassium channel gating. III: evaluation of kinetic models for activation. *J. Gen. Physiol.* 103(2):321–62

---

155. A systematic and thorough review of structures and functions of membrane proteins up to 2009.

---



# Contents

Modeling Active Mechanosensing in Cell–Matrix Interactions <i>Bin Chen, Baobua Ji, and Huajian Gao</i> .....	1
Biostructural Science Inspired by Next-Generation X-Ray Sources <i>Sol M. Gruner and Eaton E. Lattman</i> .....	33
Contemporary NMR Studies of Protein Electrostatics <i>Mathias A.S. Hass and Frans A.A. Mulder</i> .....	53
Anatomy of Nanoscale Propulsion <i>Vinita Yadav, Wentao Duan, Peter J. Butler, and Ayusman Sen</i> .....	77
Mechanisms of Autophagy <i>Nobuo N. Noda and Fuyubiko Inagaki</i> .....	101
Single-Cell Physiology <i>Sattar Taberi-Araghi, Steven D. Brown, John T. Sauls, Dustin B. McIntosh, and Suckjoon Jun</i> .....	123
Roles for Synonymous Codon Usage in Protein Biogenesis <i>Julie L. Chaney and Patricia L. Clark</i> .....	143
Biophysics of Channelrhodopsin <i>Franziska Schneider, Christiane Grimm, and Peter Hegemann</i> .....	167
Structure and Mechanism of RNA Mimics of Green Fluorescent Protein <i>Mingxu You and Samie R. Jaffrey</i> .....	187
Regulation of Rad6/Rad18 Activity During DNA Damage Tolerance <i>Mark Hedglin and Stephen J. Benkovic</i> .....	207
Structure Principles of CRISPR-Cas Surveillance and Effector Complexes <i>Tsz Kin Martin Tsui and Hong Li</i> .....	229
Structural Biology of the Major Facilitator Superfamily Transporters <i>Nieng Yan</i> .....	257



Specification of Architecture and Function of Actin Structures by Actin Nucleation Factors <i>Colleen T. Skau and Clare M. Waterman</i> .....	285
Structural Symmetry in Membrane Proteins <i>Lucy R. Forrest</i> .....	311
The Synaptic Vesicle Release Machinery <i>Josep Rizo and Junjie Xu</i> .....	339

## Index

Cumulative Index of Contributing Authors, Volumes 40–44 .....	369
---	-----

## Errata

An online log of corrections to *Annual Review of Biophysics* articles may be found at  
<http://www.annualreviews.org/errata/biophys>